Assessing the characteristics and drivers of compound flooding events around the UK coast

Alistair Hendry[1], Ivan D. Haigh[1], Robert J. Nicholls[2], Hugo Winter[3], Robert Neal[4], Thomas Wahl[5], Amélie Joly-Laugel[3] and Stephen E. Darby[6]

[1] Ocean and Earth Science, University of Southampton, National Oceanography Centre Southampton, University of Southampton, Waterfront Campus, European Way, Southampton, SO14 3ZH, United Kingdom.

[2] School of Engineering, University of Southampton, Highfield, Southampton, SO17 1BJ, United Kingdom.

[3] Natural Hazards and Environmental Group, EDF Energy R&D UK Centre, London, UK

[4] Department of Weather Science, Met Office, Exeter, UK

[5] Civil, Environmental, and Construction Engineering, National Center for Integrated Coastal Research, and Sustainable Coastal Systems Cluster, University of Central Florida, 12800 Pegasus Drive, Suite 211, Orlando, FL 32816-2450, USA.

[6] Geography and Environmental Sciences, University of Southampton, Highfield, Southampton, SO17 1BJ, United Kingdom.

Corresponding author: Alistair Hendry (A.Hendry@soton.ac.uk)

Abstract

In low-lying coastal regions, flooding arises from oceanographic (storm surges plus tides and/or waves), fluvial (increased river discharge) and/or pluvial (direct surface runoff) sources. The adverse consequences of a flood can be disproportionately large when these different sources occur concurrently, or in close succession, a phenomenon that is known as 'compound flooding'. In this paper, we assess the potential for compound flooding arising from the joint occurrence of high storm surge and high river discharge around the coast of UK. We hypothesize that there will be spatial variation in compound flood frequency, with some coastal regions experiencing a greater dependency between the two flooding sources than others. We map the dependence between high skew surges and high river discharge, considering 326 river stations linked to 33 tide gauge sites. We find that the joint occurrence of high skew surges and high river discharge occurs more frequently during the study period (15-50 years) at sites on the south-west and west coasts of the UK (between 3 and 6 joint events per decade), compared to sites along the east coast (between 0 and 1 joint events per decade). Second, we investigate the meteorological conditions that drive compound and non-compound events across the UK. We show, for the first time, that spatial variability in the dependence and number of joint occurrences of high skew surges and high river discharge is driven by meteorological differences in storm characteristics. On the west coast of the UK, the storms that generate high skew surges and high river discharge are typically similar in characteristics and track across the UK on comparable pathways. In contrast, on the east coast, the storms that typically generate high skew surges are mostly distinct from the types of storms that tend to generate high river discharge. Third, we briefly examine how the phase and strength of dependence between high skew surge and high river discharge is influenced by the characteristics (i.e. flashiness, size, elevation gradient) of the corresponding river catchments. We find that high skew surges tend to occur more frequently with high river discharge at catchments with a lower base flow index, smaller catchment area and steeper elevation gradient. In catchments with a high base flow index, large catchment area and shallow elevation gradient the peak river flow tends to occur several days after the high skew surge. The previous lack of consideration of compound flooding means that flood risk has likely been underestimated around UK coasts, particularly along the southwest and west coasts. It is crucial that this is addressed in future assessments of flood risk and flood management approaches.

Key words: Compound flooding, coastal flooding, fluvial flooding, storm surge, river discharge, UK.

1. Introduction

Flooding is the most dangerous and costly of natural disasters (Pall et al., 2011). From 1980 to 2013, floods accounted for more than $1 trillion in losses and resulted in at least 220,000 fatalities globally (Munich Re, 2017). More than 50% of these deaths and a large proportion of the economic losses occurred in densely populated low-lying coastal regions. Globally, coastal areas are home to more than 600 million people and constitute strategic economic centres (McGranahan et al., 2007). Recent flood events, for example, Cyclone Nargis in Myanmar (Fritz *et al.*, 2009), Hurricane Katrina in the US (Jonkman *et al.*, 2009), flooding in the UK over the winter of 2013/14 (Haigh et al., 2016), and Hurricane Harvey in the US (Emanuel, 2017) have demonstrated the ever-present threat of serious flood impacts in coastal regions despite improvements in levels of flood protection and advancements in flood forecasting and warnings. Furthermore, coastal flooding is a growing threat due to sea-level rise and changes in storminess (Nerem, *et al.*, 2018, Church et al., 2013), ongoing vertical land movement (Brown and Nicholls, 2015), and rapid population growth and accompanying development in flood-exposed areas (Brown *et al.*, 2018, Hallegatte *et al.*, 2013).

Flooding in coastal regions arises from four main source mechanisms: (1) storm surge combined with high astronomical tide (storm-tides); (2) local or remotely (swell) generated waves; (3) river discharge (fluvial); or (4) direct surface runoff (pluvial). The first two sources are oceanographic in origin, while the latter two mainly arise from heavy precipitation, but can also arise from snow melt. Most existing flood risk assessments consider these four main drivers of flooding separately. However, in coastal regions floods are often caused by more than just one factor, because they may be naturally correlated (i.e., with storms). Furthermore, the adverse consequences of a flood can be greatly exacerbated when the oceanographic (storm-tides and waves), fluvial, and/or pluvial drivers occur concurrently or in close succession (i.e., a few hours to days apart). Depending on local characteristics (which influence lag times between variables), this can result in disproportionately extreme events, referred to as ‘compound flood events’. Compound events are defined by the Intergovernmental Panel on Climate Change (Seneviratne *et al.*, 2012) as: *(1) two or more extreme events occurring simultaneously or successively; (2) combinations of extreme events with underlying conditions that amplify the impact; (3) combinations of events that are not themselves extremes but lead to an extreme event when combined.* Zscheischler et al. (2018) define compound events as *the*

combination of multiple drivers and/or hazards that contributes to societal or environmental risk. With the potential to create considerable destruction, the World Climate Research Program (WCRP) Grand Challenge on Extremes has recently identified compound events as an international research priority (Zscheischler *et al.*, 2018). In this paper we assess the potential for compound flooding arising from the joint occurrence of high storm surges and high river discharges around the coast of UK.

A recent example of compound flooding occurred during Hurricane Harvey in 2017. Record breaking rainfall, river discharge and runoff, combined with a moderate but long-lasting storm surge, resulted in disastrous flooding in Houston (Emanuel, 2017). It was the second costliest natural disaster in US history (NOAA, 2018). Hurricane Irma in 2017 was also a prime example of compound flooding, where significant flooding occurred along the St. Johns River in Jacksonville, as a result of a combined storm surge and extensive rainfall runoff (Cangialosi, Latto and Berg, 2017). Compound flooding can also arise from extra-tropical storms. For example, a storm surge on the Adriatic coast of Italy obstructed large amounts of freshwater runoff (generated by the same storm) from draining, causing major compound flooding in Ravenna, Italy (Bevacqua *et al.*, 2017). It is now recognised that by not considering compound flooding, the risk to these locations and elsewhere had been, and continues to be, greatly underestimated (Wahl et al., 2018).

In recent years there has been an increase in the number of studies that have started to investigate compound flood sources and events. The majority of these studies have been undertaken on a small spatial scale for specific localised regions, e.g., Fuzhou City, China (Lian *et al.,* 2013); Tsengwen River basin, Taiwan (Chen and Liu, 2014); Hudson River, USA (Orton *et al.*, 2015); Shoalhaven River, Australia (Kumbier *et al.*, 2018); the Rhine delta, Netherlands (Kew *et al.*, 2013 and Khanal *et al.*, 2018); Brest, France (Mazas and Hamm, 2017); Santander, Spain (Rueda *et al.*, 2016); Ravenna, Italy (Bevacqua *et al.*, 2017) and the River Trent, the Yare Basin, the River Ancholme, the River Taff and Lewes, East Sussex in the UK (Granger, 1959; Mantz and Wakeling, 1979; Thompson and Law, 1983; Samuels and Burt, 2002; and White, 2007, respectively). These studies have typically examined the dependence between two source variables only, such as storm surge (or storm-tide) and river discharge, between storm surge and waves, or between storm surge and rainfall (as a proxy for runoff). Larger-scale assessments of compound flood events have been undertaken more recently for Australia (Zheng et al., 2013 and Wu *et al.*, 2018), the USA (Wahl et al., 2015), the UK (Svensson and

Jones, 2002, 2004) and Europe (Petroliagkis *et al.,* 2016; Paprotny *et al.,* 2018). Recently, Ward et al. (2018) assessed the dependence between coastal and river flooding on a quasi-global scale, using observational datasets, and Marcos et al. (2019) examined the dependence between extreme storm surges and wind waves along the global coasts using outputs from numerical models.

This paper focuses on the UK, where coastal flooding is ranked as the second highest risk for causing civil emergency in the Government's National Risk Register (Cabinet Office, 2015). A series of studies in the 1990s and early 2000s, commissioned and funded by the Department for Environment Food and Agricultural Affairs (DEFRA), examined the dependence between coastal and river flooding around the UK coast (e.g., Hawkes *et al.*, 2002; Svensson and Jones, 2002, 2004; Hawkes and Svensson, 2003; Hawkes, 2005; Hawkes, Svensson and Surendran, 2005). These investigations found that large storm surges are more likely to coincide with high river discharge events at sites on the west coast than the east coast of the UK. Petroliagkis *et al.* (2016) analysed the dependence between storm surge, wave height and river flow at selected sites around Europe, including a few sites in the UK. More recently, Paprotny *et al.* (2018) examined the dependency between storm surge, river discharge and rainfall across Europe including a greater number of sites in the UK than had previously been analysed. They both identified similar spatial patterns in the strength of dependency between storm surges and river discharge across the UK. In their global study, Ward et al. (2018) also identified a west/east difference in the strength of dependence between storm surge and river discharge for the UK. However, none of these studies identified the reason(s) for this spatial variability.

The need to consider compound events in the design of flood protection schemes is strongly illustrated by the flood event on the 24th-25th December 1999 in Lymington, on the south coast of England. On the 16-17th December 1989 Lymington was flooded by high sea levels and waves, with considerable damage to 50 houses and the railway line (Ruocco et al., 2011; Haigh et al., 2015). This event was the driving force for a large upgrade of coastal flood defences for the town, including new sluice gates which allowed the Lymington River to drain at low tide, but sealed it from tidal flooding during high sea levels. However, no allowance or consideration of compound flooding appears to have been made at the time. Ten years later, on 24th December 1999, a storm generated a storm surge which did not directly cause flooding itself, because of the raised defences. However, the storm surge prevented the sluice gates from opening for prolonged periods, while large volumes of rainfall during the storm raised river flow.

Combined with the lack of drainage, this caused flooding from the river on the upstream side of the sea defences (Ruocco et al., 2011). Subsequently the Lymington flood defences were upgraded again. This event strongly highlights the importance of considering compound flooding when assessing and designing flood management.

In this paper, we build on the earlier mentioned studies and assess the potential for compound flooding arising from the joint occurrence of high storm surge and high river discharge around the coast of UK. We have three specific objectives that seek to advance the earlier studies. The first objective is to map the spatial dependence between storm surges and high river discharge around the UK, comparing different methods for quantifying the dependence between these two variables. The research question is where do compound flood events occur around the coast? Our hypothesis is that there will be a spatial variation in compound flood frequency, with some coastal regions experiencing a greater dependency between the two flooding sources than others. A key concern in regard to compound flooding is timing of the two flood sources, for example, if a surge arrives after the extreme river flow, a compound flood event may be avoided, therefore we investigate the lag between the two flood sources.

Our second objective is to investigate the meteorological conditions that drive compound and non-compound events across the UK. Svensson and Jones (2002, 2004) briefly examined storm tracks associated with joint occurrence events, but here we undertake a much more extensive meteorological analysis, and use the results from this to explain, for the first time, why large storm surges and high river discharge are more likely to coincide on the west UK coasts, compared to the east coast. The research question is which weather types favour the occurrence of compound events? Our hypothesis is that certain types of weather conditions will favour the joint occurrence of storm surge and river discharge while other weather patterns will not. This will be particularly useful for flood forecasting, and therefore will be compared to Coastal Decider, a medium- to long-range operational forecasting tool developed by The UK Flood Forecasting Centre (a collaboration between the UK Environment Agency and Met Office).

Our third and final objective is to briefly examine how the strength and phase of dependence between storm surge and river discharge are influenced by the characteristics (i.e., flashiness, size, elevation gradient) of the corresponding river catchments. We hypothesize that the lower the flashiness, the smaller the catchment area and the greater the average elevation gradient, the more likely that storm surges will occur around the same time as high river discharge.

2. Data

We used four main data types in this study, namely: (1) sea level time-series; (2) river discharge records; (3) meteorological datasets; and (4) river catchment characteristics. Those are described in the following four sub-sections. In Section 2.5 we then describe how we select the tide gauge and river discharge sites for the subsequent analysis outlined in Section 3.

2.1. Sea level data

Sea level time-series from the UK National Tide Gauge network were obtained from the British Oceanographic Data Centre (BODC; https://www.bodc.ac.uk). Data is available for 42 tide gauge sites around the UK coast, but we focus on 33 sites (see Section 2.5). Sea level records are available as hourly measurements before 1993 and quarter hourly after 1993. The longest sea level record (Newlyn [5]) starts in 1915, whilst the shortest (Portrush [20]) begins in 1995. We consider data up to the end of 2016. The data has been previously quality controlled by the BODC, with questionable values flagged as improbable, null or interpolated. Any values that were flagged as improbable or null have been removed from the analysis.

2.2. River discharge data

River discharge data was obtained from the UK's National River Flow Archive (NRFA; ttp://nrfa.ceh.ac.uk/). Data is available for more than 1,500 river gauge sites, but we focus on 326 sites (see Section 2.5). The measurements are available as daily mean rates. The longest river discharge record (Kingston, on the Thames) starts in 1883, whilst the shortest (Deerhurst on the Severn), begins in 1995. Again, we consider data up to the end of 2016. The data has been previously quality controlled by the Centre for Ecology & Hydrology (CEH), and we excluded data that was flagged as suspect.

2.3. Meteorological data

We use gridded mean sea level pressure (SLP), near-surface U and V wind and precipitable water content (PWC, entire atmosphere considered as a single layer) fields to investigate the meteorological conditions that drive compound and non-compound events. The first two variables are chosen because they are the primary variables leading to storm surges, whereas the latter is used as a proxy for rainfall. We use data from the 20th Century global meteorological Reanalysis, Version 2c (Compo *et al.*, 2011), obtained from the National Oceanic and Atmospheric Administration website (NOAA; https://www.esrl.noaa.gov/psd/data/20thC_Rean/). The fields have a spatial and temporal resolution of 2 degrees and 6 hours, respectively and are available from 1851. Whilst the spatial resolution is relatively coarse, the 20th Century Reanalysis was chosen to encompass the full time series of tide and river gauge data. Finer resolution reanalysis datasets (such as ERA-5) have shorter timeseries. We focus on the data within the area 34 ˚N to 70˚N and 60˚W to 20˚E, which encompasses the region where storms affecting the UK are generated and influence the region.

We also compare the results to Coastal Decider. This is based on probabilistic weather-pattern forecasts and helps to identify periods with an increased likelihood of coastal flooding from high sea levels around the UK. Coastal Decider uses a set of 30 distinct weather patterns (referred to as the 'Met Office weather patterns') which were derived by Neal et al. (2016) using k-means clustering techniques. These weather patterns (shown in Supplementary Figure S32) represent the large-scale meteorological conditions experienced over the UK and surrounding European area. Neal et al. (2018) used a daily historical weather pattern catalogue to show that particular weather patterns tend to relate to high sea level events at different sites around the UK, with this analysis forming the basis for Coastal Decider. Other research which relates the Met Office weather patterns to meteorologically induced hazards includes Richardson et al. (2018), who related the weather patterns to precipitation observations for the application of drought forecasting.

2.4. Catchment characteristics

We obtained or calculated river catchment characteristics from information on the NRFA website, for each of the river discharge sites we analysed. We consider three catchment characteristics as follows: (i) base flow index (BFI); (ii) catchment area; (iii) and catchment

elevation variation. The BFI is a measure of the proportion of the river runoff that derives from stored sources (Gustard, Bullock and Dixon, 1992) and gives an indication of the flashiness (how quickly a river responds to precipitation) of a catchment. The more permeable the rock and soils in a catchment, the higher the base flow. Rivers draining impervious clay catchments (with minimal lake or reservoir storage) typically have baseflow indices in the range 0.15 to 0.35, whilst chalk streams have a BFI greater than 0.9 as a consequence of the high groundwater component in the river flow. The catchment area is the size of the drainage basin of a particular river. Both the BFI and catchment area are provided directly on the NRFA website, for each catchment (NRFA; http://nrfa.ceh.ac.uk/). The catchment elevation variation is a measure of the steepness of a catchment. The NRFA provide statistics on the elevation of the minimum and maximum elevations in a catchment, along with the elevations at the 10^{th}, 50^{th} and 90^{th} percentiles of the river catchment. We calculated an elevation variation index by taking the difference between the 90^{th} and 10^{th} elevation percentiles and normalizing these about the mean of all sites; values close to 1 indicate a catchment with a steep elevation gradient and values close to 0 indicate a catchment with a gentle gradient.

2.5 Site selection

From the available datasets, described above in Sections 2.1 and 2.2, we match combinations of tide gauge and river discharge sites that satisfied the following criteria: (1) there are at least 15 years of overlapping records; and (2) daily mean river discharge is at least 5 m^3/s at the river site. Previous studies often matched river gauge sites to the nearest tide gauge sites (Paprotny et al., 2018) or every river gauge to every tide gauge site (Svensson and Jones, 2002 and 2004). However, because of the complex topography of the coastline, this doesn't always associate a river gauge site to the hydrologically-relevant tide gauge (and coast) for that river system. Therefore, we visually matched each river site to the tide gauge site nearest to the appropriate river mouth. Nine tide gauge sites ((1) Dover; (2) Newhaven; (3) Port Erin, Isle of Man; (4) St Hellier, Jersey; (5) St Marys, Isles of Scilly; (6) Stornoway, Lewis and Harris; (7) Lerwick, Shetland Islands; (8) Lowestoft; and (9) Harwich), were excluded from the analysis as there was no appropriate nearby river systems with discharge measurements, or the corresponding overlapping record length was less than 15 years for that specific combination of sites.

Following this selection, there are 326 combinations of discharge stations and tide gauges, the locations of which are shown in Figure 1, linked to 33 tide gauge sites. In Figure 1a, and

subsequent figures of this nature hereafter, river sites discharging onto the west, east and south coasts of the UK are plotted as triangles, circles and squares, respectively. There is good spatial coverage across most of the country, except in the southeast. The river sites discharging along the southeast, tend to have discharges below 5 m^3/s, or the overlapping data lengths are less than 15 years. Some tide gauge sites (e.g., Newlyn (5) and Wick [26]) are not in the near vicinity of where corresponding rivers drain into the sea. However, as storm surges have large spatial extents, they are close enough to be considered representative of the broader scale storm surge characteristics in that area.

The number of years for which overlapping data is available for both sites is also shown in Figure 1a. The tide gauge data was typically the shorter of the two sets. The mean overlapping length across all sites was 24 years, with a maximum of 50 years. Tide gauges had an average of 10 river gauges linked to them (Figure 1b), with a minimum of 1 (Newlyn [5], Fishguard [12] and Holyhead [14]) and a maximum of 37 (Immingham [31]). At some tide gauge sites, multiple sub-catchments have been used, sometimes with multiple discharge stations on the same river. Details of the location of the combination of sites and their overlapping data lengths are given in Table 1.

3. Methods

The analysis was undertaken in three main stages, each addressing one of the three study objectives outlined above. These stages are described in turn in the sections below.

3.1. Joint occurrence and dependence

Our first objective is to map the dependence between storm surge and river discharge, comparing different methods for quantifying the dependence between these two variables. For sea level we considered two parameters: (1) total still sea-level; and (2) storm surge (i.e., the meteorological component of sea level). To represent the latter, we used the skew surge parameter, which is the difference between the maximum observed high water and the maximum predicted (astronomical) high water, each tidal cycle, regardless of their timing. To extract time-series of skew surges from the sea level records at each tide gauge site, we followed the approach of Haigh *et al.* (2016). To do this, we first undertook a harmonic analysis, for each calendar year, using the T-Tide harmonic analysis package (Pawlowicz et al., 2002) with the standard 67 tidal constituents. Each observed and predicted high water was

identified, and the difference between the two was computed to give time-series of skew surges. Daily maxima total still sea level and skew surge time-series were then extracted, at each tide gauge site. The exact time of the daily maxima was retained for the meteorological analyses, described later in Section 3.2. The river discharge records were obtained in the format of daily mean values, and so no pre-processing was necessary on these records.

Extreme levels were extracted for each of the three (i.e., total sea level, skew surge and river discharge) daily time-series, at each site, using a peaks over threshold (POT) approach. We used a declustering algorithm, with a storm length of 48 hours (which is appropriate as Haigh *et al.* (2016) found storms in the UK typically affect sea level for 3.5 days) to guarantee independent events. We varied the threshold at each site to ensure that each of the three time-series had on average 2.3 to 2.5 extreme levels per year. This threshold range ensured that: (1) we had enough data points to estimate dependence between the variables reliably; and (2) the threshold was high enough for the exceedances to be considered 'extreme' (Svensson and Jones, 2005). The average thresholds across all sites were the 99^{th}, 99.1^{th}, and 99.2^{th} percentiles for total sea level, skew surge and river discharge, respectively.

We then used two different approaches to assess the dependence between total sea level or skew surge, with river discharge. The first approach we term hereafter the 'dependence method'. Here, we measure dependence between the daily maximum total sea-level/skew surge and discharge time-series using Kendall's Rank Correlation τ (Kendall, 1938), which, unlike the Pearson's Correlation Coefficient, captures non-linear relationships. Significance was assessed at $\alpha = 0.05$ (i.e., 95% confidence level), using corresponding p values estimated from exact permutation distributions. We also repeat the analysis using time-lags from −5 to +5 days. For example, for daily maximum skew surge we select corresponding daily maximum discharge values with time lags of −5, −4, −3, −2, −1, 0, +1, +2, +3, +4, and +5 days. This is to allow for that fact that when a storm approaches the coast, for example, it might first generate a high storm surge, before travelling inland and generating high precipitation and therefore elevated river discharge sometime afterwards.

The second approach we term hereafter the 'joint occurrence method'. Here we simply count the number of times extreme total sea levels events, or skew surges events, above the chosen threshold for that site, occurred on the same day as extreme river discharge. Each pair of sites have varying overlapping data lengths. Therefore, to standardise the results, the number of joint

occurrences per decade were determined. Again, we repeat the analysis but lag the discharge using time-lags of -5 to +5 days.

To illustrate the approaches, time-series of daily maximum skew surges are plotted against records of daily maximum river-discharge at 0-day lag for Devonport (southwest coast) and Whitby (east coast) in Figure 2a and 2b, along with the two percentile thresholds. At Devonport there are 9 occasions (red dots in Figure 2a) when extreme skew surges occur on the same date as extreme river discharges, whereas at Whitby (Figure 2b) there are no coincident events.

3.2. Meteorological analysis

Our second objective is to investigate the meteorological conditions that drive compound (i.e., joint occurrence of high skew surges and large river discharge) and non-compound events (i.e., high skew surge or high river discharge only) events across the UK. For each site, we extract fields of SLP, wind speed and PWC for the 6-hour period closest to the peak of each: (1) extreme total sea level or skew surge event (i.e., all the events in zone 1 on Figure 2); (2) each joint occurrence event (i.e., all the events in zone 2 on Figure 2); and (3) each extreme river flow event (i.e., all the events in zone 3 on Figure 2). For each site, and each of these three types of events, we derive composite plots of SLP, wind speed and PWC, by taking an arithmetic mean and standard deviation of the data at each hindcast grid cell, through the time of the corresponding events. The composite plots thus represent the mean (with variance around the mean) conditions of the storms that generate compound and non-compound events. We also digitised the tracks of all responsible storms, for the three different event types, using the storm tracking algorithm developed by Haigh *et al*. (2016). This captures the location of the storm centre for each 6-hourly time step of the metrological reanalysis, from cyclogenesis to storm dissipation or when the storm leaves the area of interest (defined above). We calculate the mean storm track for each event type, at each site. This allows us to compare and contrast the weather patterns related to the storms which caused the compound and non-compound events.

3.3. Catchment correlations

Our final objective is to briefly examine how the strength and phase of dependence between total sea level or skew surge and river discharge is influenced by the characteristics of the corresponding river catchments. To do this we calculate correlation coefficients between the

strength of dependence (or number of joint occurrences per decade) and the maximum phase lag, with our three selected catchment variables (BFI, catchment area and catchment elevation variation). Again, significance was assessed at $\alpha = 0.05$. We hypothesize that the lower the BFI, the smaller the catchment area and the greater the average elevation gradient, the more likely that high total sea levels or skew surges will occur around the same time as high river discharge. The higher the BFI, the larger the catchment area and the gentler the elevation gradient of the catchment, the more likely it is that high river discharge will occur several days after high total sea level or skew surge, for the sites closest to the coast.

4. Results

4.1 Dependence and joint occurrences

We used two methods to assess the dependence between high total sea level or high skew surge with high river discharge, across the 326 combinations of discharge stations and tide gauge sites. The results of the first method, the dependence method, are shown in Figures 3a and 4a for daily maximum total sea level and daily maximum skew surge, respectively, with daily maximum river discharge, for 0-day lag. As expected, there is generally greater dependence between skew surges and river discharge (Figure 4a), than between total sea level and river discharge (Figure 3a). This is because total sea levels are strongly influenced by the deterministic tidal component, around the majority of the coastline of the UK (Haigh *et al.*, 2016). Interestingly, the dependence is stronger for total sea levels for sites linked to tide gauges in the northern Irish Sea (e.g., Portrush [20] and Bangor [19] in North Ireland and Portpatrick [21] and Millport [22] in Scotland), and this is most likely because tidal range is small here, and not such a dominant factor on total sea levels, compared to other sites. A clear spatial variation in the dependence between high sea levels or skew surges with high river discharge is evident in Figures 3a and 4a. For many of the sites along the south-west and west coasts of the UK, τ typically ranges from 0.1 to 0.35 whilst along the east coast this drops to 0.0 to 0.15. The greatest dependence is found at river gauges linked to the Millport [22] and Portpatrick [21] tide gauges in southwestern Scotland. The lowest dependence is located at river gauges near Cromer [32] on the East Coast. Two river sites linked to the Bangor [19] tide gauge in Northern Ireland show negative dependence.

We also calculated the dependence between daily maximum total sea level or skew surge and daily maximum river discharge using time lags from −5 to +5 days. The results for high skew surge and high river discharge are shown in Supplementary Figures S1a to S11a for all sites. Dependence is typically weak until -1-day lag. Interestingly the dependence is higher for +1 to +5-day lags, compared to -5 to -1-day lags. This is illustrated in Figure 5 for the six river sites closest to the tide gauges of Bournemouth [2], Devonport [4], Workington [18], Ullapool [24], Whitby [30] and Cromer [32]. The distributions are typically skewed to the right, and this is probably because river levels remain elevated for several days after a storm event. The lag day when there is the maximum dependence between daily maximum skew surge and daily maximum river discharge is shown in Figure 6a, for all sites. Interestingly, 42 inland sites (13% of the 326 sites) on the east coast have a maximum correlation at -1-day lag. The majority of the sites (188; 58%) have maximum correlation at 0-day lag. Sites on the south-west and west coast typically have maximum correlations between +1 and +5 days. The number of sites on each day of maximum dependence can be seen in Table 2. The sites with maximum correlations at +4 and +5-day lag are mostly situation in the Severn River, which has a large catchment area (see Section 4.3).

The results for the second method, the joint-occurrence method, are shown in Figures 3b and 4b for high total sea levels and high river discharge, and high skew surges and high river discharge, respectively, at 0-day lag. The spatial patterns are very similar to those of the daily dependence results. For many of the sites along the south-west and west coasts of the UK, there are a higher number of joint occurrences between high skew surges and high river discharge (between 3 and 6 joint events per decade), than for sites along the east coast (between 0 and 1 joint events per decade). Sites with the largest numbers of joint occurrences (5 to 6 events per decade) include river discharge sites linked to Millport [22], Workington [18], Mumbles [10], Devonport [4] and Bournemouth [2] tide gauges. There are several sites along the south-west and west coasts which show low (< 1 event per decade) or zero joint occurrences at 0-day lag. These include river discharge sites linked to tide gauges at Heysham [17] and Portsmouth [1] in England, Bangor [19] in Ireland, Barmouth [13] and Milford Haven [11] in Wales, and Portpatrick [21], Ullapool [24] and Kinlochbervie [25] in Scotland. Interestingly, there is large variation on a regional/local scale, particularly in areas which mostly have high numbers of joint occurrences. For example, at many sites around the Bristol Channel, the number of joint occurrences varies between 1 to 4 per decade, at river discharge sites less than 80 km apart.

The number of sites with joint occurrences per decade between (i) total water level and river discharge; and (ii) skew surge and river discharge can be seen in Table 3.

The lag day when there are the maximum number of joint occurrences between high skew surge and high river discharge are shown in Figure 6b, for all study sites. The results are similar to those seen for the daily maximum dependence approach (Figure 6a). Inland sites on the east coast typically have a maximum number of joint occurrences at -1 to -3 days lag, whereas several sites on the west coast have a maximum number of joint occurrences at +1 to +5 days lag.

4.2 Meteorological analysis

We now investigate the meteorological conditions that drive compound (i.e., joint occurrence of high skew surges and large river discharge) and non-compound events (i.e., high skew surge or high river discharge only) events across the UK. We focus here on skew surge, rather than total sea level, as the dependence between skew surges and river discharge is stronger. At each of the 326 river discharge sites, we have derived composite plots of SLP, wind speed and PWC through the time of the events that have led to: (1) high skew surge events only; (2) joint occurrence events; and (3) high river discharge events only. To illustrate the results of this component we focus on two contrasting sites: Devonport [4] on the UK southwest coast where high storm surges and high river discharge have occurred at similar times in the past (Figure 2a); and Whitby [30] on the UK east coast, where high storm surges have never occurred (during the period of record) at times of high river discharge (Figure 2b). Examples of 8 other sites are shown in Supplementary Figures S23 to S30.

Composite plots are shown in Figures 7 and 8 for Devonport [4] and Whitby [30], respectively, for SLP (left column), wind speed (central column), and PWC (right column) for the events that had: (1) high skew surge only (top row); (2) both high skew surge and high river discharge (middle row); and (3) high river discharge only (bottom row). The number of events recorded for each type is listed, and the average standard deviation (SD), across all grid cells, is also reported. The latter gives an indication of the spread of the spatial patterns across all the corresponding events (i.e., a low SD indicates that the storms across all events have very similar spatial patterns).

At Devonport (Figure 7), the meteorological patterns in SLP are similar across the three event types. All three event types feature a low-pressure system to the northwest of Ireland (Figures 7a, 7d and 7g), with strong south-westerly winds affecting the southwest coast. As expected, the wind speed is more intense along the south coast for the skew surge only (Figure 7b) and joint event types (Figure 7e), compared to the river discharge only events (Figure 7g). The differences in PWC patterns are more pronounced. There is low PWC over the southwest for the surge only events (Figure 67c), and higher PWC for the joint and river only event types (Figure 7f and 7j). The composite plot of PWC is characterised by a higher SD for surge only events (e.g., there is more spread across the range of events) in comparison to the joint and river only event types.

In contrast, at Whitby, the meteorological patterns in SLP are very different across the two event types (note, no joint high skew surge and high river discharge were observed here) (Figure 8), showing that the storms that lead to high skew surges are distinct from the storms that lead to high rainfall and therefore river discharge. For high skew surge only events, the storm centre is situated over Scandinavia (Figure 8a), producing strong north-westerly winds across the North Sea (Figure 8b). PWC is low for the entire east coast (Figure 8c). For high river only events, a weaker low-pressure system is centred over central UK (Figure 8g). The wind speeds are therefore low on the East Coast (Figure 8h). However, the PWC is high over much of the UK.

The results for other sites are similar (Supplementary Figures S23 to S30). For sites on the west coast of the UK, the storms typically have similar SLP characteristics between the three event types. Whereas, for sites on the east coast, the storms are more distinct.

We also digitised the tracks of the storms responsible for each of the three event types, at these two selected sites. These storm tracks are shown in Figure 9 for Devonport (upper panels) and Whitby (lower panels). The mean storm tracks are overlaid, in each instance. At Devonport, the mean storm tracks are typically similar, moving in an easterly north-easterly direction and cross over the north, or just to the north of Scotland (Figures 9a, 9b and 9c). The slight variation is likely due to the resolution of the average track. In contrast, at Whitby, the mean storm tracks for the high skew surge events and high river discharge events are very different. The mean storm track for the high skew surge events pass to the north of Scotland (Figure 9d), while the high river only events cross central UK (Figure 9f), all in a west to east direction.

4.3 Localised correlations

The analysis of weather types (described in Section 4.2) has helped to explain national scale spatial variations in the occurrence of compound events (i.e., the west/east difference shown in Figure 4), but to understand variations locally we need to consider other variables. We therefore briefly assess here, how the strength and phase of dependence between skew surge and river discharge is influenced by the characteristics of the corresponding river catchments.

The three selected catchment characteristics (BFI, catchment area and catchment elevation variation) are plotted in Figures 10a, 10b and 10c, respectively. The river sites that drain onto the central south coast typically have the greatest BFI (nearly 1, i.e. extremely porous chalk), whilst those on the north west coast typically have the lowest (0-0.2, i.e. predominately clay soils) (Figure 10a). Catchments are largest on the Severn River, the River Bann in Northern Ireland and the east coast of Scotland, whereas smaller catchments are found in Cornwall, West Scotland and around Weymouth (Figure 10b). The largest elevation variation is seen on the River Spey in Scotland and altitude variation is low across the east coast of UK between Immingham and Dover (Figure 10c). Visually, there is no obvious strong spatial correlation between any of the three catchment characteristics (Figure 10) and either the rank correlation between daily maximum skew surge and daily maximum river discharge (Figure 4a) or the number of joint occurrences per decade between extreme skew surge and extreme river discharge (Figure 4b).

The rank correlation for daily maximum skew surge and daily maximum river discharge (at 0-day lag) is plotted against the three catchment characteristics for each site in Figures 11a, 11b and 11c. The day of maximum lag for the rank correlation is plotted against the three catchment characteristics for each site in Figures 11d, 11e and 11f. Corresponding correlation coefficients (CC) are listed in Table 4, first for all sites and then just the river sites closest to the 33 tide gauge sites. There is a negative correlation (CC = -0.5, significant at 95%) between dependence and BFI. This is in line with our hypothesis that the lower the BFI of the site (e.g., the flashier the catchment), the more likely that high skew surges will occur around the same time as high river discharge. There is a statistically significant negative correlation (CC = -0.31) between dependence and catchment area. Again, this is in line with our hypothesis that high skew surges

are more likely to occur around the same time as high river discharge in small catchments. There is a weak but statistically significant positive correlation (CC = 0.16) between dependence and catchment altitude variation. Again, this is in line with our hypothesis that the steeper the catchment, the more likely that high skew surges will occur around the same time as high river discharge. The correlation is higher (CC = 0.34, significant at 95%) for just the 33 river sites closest to each tide gauge site. The correlations between the three catchment characteristics and the day of maximum lag are not as strong (Table 2; Figures 11d, e and f). There is a weak statistically significant correlation (CC = 0.21, significant at 95%) between day of maximum lag and BFI. Sites with larger BFI typically have larger positive lags. There is also a weak, statistically significant, correlation (CC = 0.11, significant at 95%) between day of maximum lag and catchment area. Sites with large catchment area typically have larger positive lags.

5. Discussions

In this paper we have assessed the potential for compound flooding arising from the joint occurrence of extreme total water level or skew surge and river discharges around the coast of UK. Like earlier studies (i.e., Svensson and Jones, 2002, 2004; Petroliagkis *et al.*, 2016; Paprotny *et al.*, 2018) we have identified that the joint occurrence of high skew surges and high river discharge occurs more frequently on the south-west and west coasts of the UK, compared to the east coast. However, here we have been able to show, for the first time, that this spatial variability is driven by meteorological differences in storm characteristics. On the west coast of the UK, the storms that generate high skew surges and high river discharge, are typically similar in characteristics (i.e., there is a low-pressure system to the northwest of Ireland with strong south-westerly winds affecting the southwest coast) and track across the UK on comparable pathways. In contrast, on the east coast, the storms that typically generate high skew surges (i.e., when there is a low pressure over Scandinavia producing strong north-westerly winds across the North Sea) are distinct from the types of storms that tend to generate high river discharge in this area (i.e., when there is a weaker low-pressure system over central UK).

We also identified, for the first time, relationships across the UK between the strength and phase of the dependence between high skew surge and high river discharge and the characteristics of the corresponding river catchments. We find that high skew surges tend to

occur more frequently with high discharge in catchments with a lower base flow index, smaller area and steeper elevation gradient. In catchments with a high base flow index, large area and shallow elevation gradient the peak river flow tends to occur several days after high skew surge. We also found that for inland river discharge sites on the east coast, the maximum number of joint occurrences happens when river discharge occurs -1 days before peak skew surge. This is because the maximum storm surge in the North Sea occurs after the storm has crossed the North Sea into Scandinavia, whereas the high rainfall occurs a day earlier when the storm is centred over the UK.

The key concern for compound flooding is when estuaries or coastal regions experience both high storm surge and high river discharge around the same time (i.e., 0-day lag), which is likely to lead to disproportionately large adverse flood consequences. Of the 33 tide gauge sites considered, dependence between high skew surge and high river discharge is maximum at 0-day lag at 19 sites (for the river discharge station closest to these sites; see Supplementary Figure S31). At most other sites, high river discharge occurs between +1 and +5 days after peak skew surge, and therefore compound flooding is not as much a concern. However, there are still important implications for flood management and emergency response if a large fluvial flood occurs several days after a major coastal flood, as this is likely to stretch emergency services.

The meteorological analysis we have undertaken, indicates subtle differences in the types of storms that tend to generate compound events, compared to non-compound events, particularly for sites on the west coast of the UK (see Figure 6). As compound events tend to exacerbate the adverse consequences of a flood, it is vital they are forecasted accurately, and appropriate warning is provided. Furthermore, the best response to a compound event might differ from a non-compound event. Therefore, to be able to accurately forecast that an event might be a compound event, as opposed to a non-compound event, is crucial. With these insights and improvement in forecast opportunities discussed below, these aspects of emergency response should be analysed in more detail.

Here, we use the same daily historical weather pattern catalogue as Neal *et al.* (2018) and Richardson *et al.* (2018) to calculate the modal weather pattern at each site for: (1) high skew surge events only; (2) joint occurrence events, and; (3) high river discharge events only. This is done in order to briefly assess whether Coastal Decider could be expanded to give early

warnings of events with the potential to generate compound flooding from both high sea level and high river discharge. Results are shown in Figure 12. Nearly all the events are dominated by the higher numbered weather patterns, which tend to be the more stormy types and which are most likely to occur in the winter. Clear distinctions are found along coastal regions. Weather pattern 30 occurs for sites along the southwest and west UK coast, for each of the three types of events. This is one of the stormiest weather patterns with a large depression situated to the north of Scotland. This causes a strong westerly flow across the UK with frontal rainfall being particularly heavy in western parts of the UK. Weather pattern 20 is dominant along the central west coast, particularly from the Bristol Channel northwards. This weather pattern is similar to weather pattern 30, but with the depression centre further north, therefore shifting the wind and rain impacts further north. Sites in Scotland typically feature weather patterns 20 (cyclonic westerly) and 21 (cyclonic south-westerly). Along the east coast high skew surge and river discharge events experience different weather patterns with pattern 14 (cyclonic northerly) generally being seen during high skew surge events compared to patterns 11 (low pressure centred over the UK), 24 (southerly tracking cyclone centred over the North Sea) and 30 (very cyclonic westerly) which are generally related to high river events. These results indicate that it may be possible to extend the forecasting capability of Coastal Decider to also include indications for the likelihood of compound events. Small scale weather features will need to be included in the mean composites for each weather pattern (e.g., weather pattern 30, which is a very stormy cyclonic south westerly type, will have a mean composite that is formed from many subtle variations in the overall broad-scale stormy south westerly flow; this means that the small scale (and perhaps rarer) features will still be represented within a broader scale weather pattern).

So far, we have just considered high water levels which produce the potential for flooding. In periods of high run-off in the UK such as 1998, 2000 and 2007 floods happened repetitively near the tidal limit of rivers due to tidal locking at high tide such as the floods in Lewes in 2000 (White, 2007). However, these may not be compound events as defined here. To briefly assess the extent of flooding during compound events, we compared the dates of joint occurrences at Devonport (which had a higher number of joint occurrences per decade) with reports of coastal flooding in the SurgeWatch database (Haigh *et al.*, 2015, 2017). SurgeWatch records the social, economic and environmental consequences of 330 coastal floods that have impacted the UK in the last 100 years. Of the 9 joint occurrence events when there was both high skew surge and high river discharge observed at Devonport, 7 events had reports of coastal flooding.

Events with significant flooding included: 24th-25th December 1999, which caused extensive flooding in Lymington, Dorset, as discussed below; and the 14th February 2014 storm which led to the destruction of the main railway line in Dawlish (Devon Maritime Forum, 2014) (note, this event also had large waves). No flooding was reported for the Great Storm of 15th-16th October 1987 (Burt and Mansfield, 1988). There was extensive wind damage during this event to the UK, but little coastal flooding because the event coincided with neap tides.

As stated earlier, compound flooding can occur not only during two (or more) extreme events, but also when just one flood source is extreme (for example, extreme river discharge combines with a moderate storm surge); or when two moderate flooding sources combine to create a flood event. It should be noted, that the latter two types of compound flooding involving moderate events were beyond the scope of this paper and so were not considered in our methods. These types of events are important however and need to be recognised in future studies into flood risk.

6. Conclusions

This paper has assessed the potential for compound flooding arising from the joint occurrence of extreme total water level or skew surge and river discharges around the coast of UK. We found that the joint occurrence of high skew surges and high river discharge occurs more frequently during the study period (15-50 years) at sites on the south-west and west coasts of the UK (between 3 and 6 joint events per decade), compared to sites along the east coast (between 0 and 1 joint events per decade). We showed, for the first time, that the spatial variability in the dependence and number of joint occurrences of high skew surges and high river discharge is driven by meteorological differences in storm characteristics. On the west coast of the UK, the storms that generate high skew surges and high river discharge are typically similar in characteristics and track across the UK on comparable pathways. In contrast, on the east coast, the storms that typically generate high skew surges are mostly distinct from the types of storms that tend to generate high river discharge. We found that high skew surges tend to occur more frequently with high river discharge at catchments with a lower base flow index, smaller catchment area and steeper elevation gradient. In catchments with a high base flow index, large catchment area and shallow elevation gradient the peak river flow tends to occur several days after the high skew surge. The previous lack of consideration of compound flooding means that flood risk has likely been underestimated around UK coasts,

particularly along the southwest and west coasts. Furthermore, the additional damages caused due to compound events are unknown. It is therefore crucial that this is addressed in future assessments of flood risk and flood management approaches.

Author contribution: AH and IDH conceived, planned and carried out the analysis and interpretations. RJN aided as an expert in coastal flooding. HW provided guidance on extreme value statistics. RN and AJL provided the knowledge on the meteorological component. TW offered his expertise in compound flooding. SED added his knowledge of fluvial processes. The manuscript was prepared by AH and IDH with contributions from all co-authors.

Competing interests: The authors declare that they have no conflict of interest.

Data Availability: This study relies entirely on publicly available data, described in Section 2. Dependence and joint occurrence results can be seen in Table S1 in the supplementary material.

Acknowledgements: We would like to thank EDF Energy R&D Centre UK and the Southampton Marine and Maritime Institute (SMMI) for funding this research. IDH acknowledges the NERC grant CHANCE (NE/S010262/1). We would also like to thank the data providers: the British Oceanographic Data Centre; and the National River Flow Archive for supplying the sea level and river data, respectively. In addition, we'd like to thank the Earth Systems Research Laboratory (ESRL, NOAA) for providing the 20th Century V2c meteorological reanalysis.

References

Ansell, T. J. *et al.* (2006) 'Daily mean sea level pressure reconstructions for the European-North Atlantic region for the period 1850-2003', *Journal of Climate*, 19(12), pp. 2717–2742. doi: 10.1175/JCLI3775.1.

Bevacqua, E. *et al.* (2017) 'Multivariate statistical modelling of compound events via pair-copula constructions: Analysis of floods in Ravenna (Italy)', *Hydrology and Earth System Sciences*. Copernicus GmbH, 21(6), pp. 2701–2723. doi: 10.5194/hess-21-2701-2017.

Brown, S., & Nicholls, R. J. (2015). Subsidence and human influences in mega deltas: The case of the Ganges-Brahmaputra-Meghna. *Science of the Total Environment*, *527–528*, 362–374. https://doi.org/10.1016/j.scitotenv.2015.04.124

Brown, S. *et al.* (2018). Quantifying Land and People Exposed to Sea-Level Rise with no Mitigation and 1.5∘C and 2.0∘C Rise in Global Temperatures to Year 2300, *Earth's Future*, *6*. https://doi.org/10 .1002/2017EF000738

Burt, S. D. and Mansfield, D. . (1988) 'The Great Storm of 15-16 October 1987', *Weather*, 43, pp. 90–110.

Cabinet Office (2015) *National Risk Register of Civil Emergencies*. Available at: https://www.gov.uk/government/uploads/system/uploads/attachment_data/file/419549/20150331_2015-NRR-WA_Final.pdf (Accessed: 13 March 2017).

Cangialosi, J. P., Latto, A. S. and Berg, R. (2017) *National Hurricane Center Tropical Cyclone Report: Hurricane Irma (AL112017)*. Available at: https://www.nhc.noaa.gov/data/tcr/AL112017_Irma.pdf (Accessed: 7 November 2018).

Chen, W. B. and Liu, W. C. (2014) 'Modeling flood inundation induced by river flow and storm surges over a river basin', *Water (Switzerland)*. Multidisciplinary Digital Publishing Institute, 6(10), pp. 3182–3199. doi: 10.3390/w6103182.

Church, J.A., P.U. Clark, A. Cazenave, J.M. Gregory, S. Jevrejeva, A. Levermann, M.A. Merrifield, G.A. Milne, R.S. Nerem, P.D. Nunn, A.J. Payne, W.T. Pfeffer, D. Stammer and A.S. Unnikrishnan, 2013: Sea Level Change. In: Climate Change 2013: The Physical Science Basis. Contribution of Working Group I to the Fifth Assessment Report of the Intergovernmental Panel on Climate Change [Stocker, T.F., D. Qin, G.-K. Plattner, M. Tignor, S.K. Allen, J. Boschung, A. Nauels, Y. Xia, V. Bex and P.M. Midgley (eds.)]. Cambridge University Press, Cambridge, United Kingdom and New York, NY, USA.

Compo, G. P. *et al.* (2011) 'The Twentieth Century Reanalysis Project', *Quarterly Journal of the Royal Meteorological Society*, 137(654), pp. 1–28. doi: 10.1002/qj.776.

Devon Maritime Forum (2014) *Reviewing the impacts, responses and resilience of people and places in Devon to the winter storms of 2013/2014*.

Emanuel, K. (2017) 'Assessing the present and future probability of Hurricane Harvey's rainfall.', *Proceedings of the National Academy of Sciences of the United States of America*. National Academy of Sciences, 114(48), pp. 12681–12684. doi: 10.1073/pnas.1716222114.

Fritz, H. M. *et al.* (2009) 'Cyclone Nargis storm surge in Myanmar', *Nature Geoscience*. Nature Publishing Group, 2(7), pp. 448–449. doi: 10.1038/ngeo558.

Granger, C. W. J. (Clive W. J. (1959) 'Estimating the probability of flooding on a tidal river', *Journal of Institution of Water Engineers*. Cambridge University Press, 13, pp. 165–174. Available at: http://dl.acm.org/citation.cfm?id=766904 (Accessed: 21 March 2017).

Gustard, A., Bullock, A. and Dixon, J. M. (1992) 'Low flow estimation in the United Kingdom', *Institute of Hydrology, Wallingford*, (108), pp. 1–292. Available at:

http://nora.nerc.ac.uk/id/eprint/6050/1/IH_108.pdf (Accessed: 19 January 2018).
Haigh, I. D. *et al.* (2015) 'A user-friendly database of coastal flooding in the United Kingdom from 1915-2014', *Scientific Data*. Nature Publishing Group, 2, pp. 1–13. doi: 10.1038/sdata.2015.21.
Haigh, I. D. *et al.* (2016) 'Analysis : Spatial and temporal analysis of extreme sea level and storm surge events around the coastline of the UK', pp. 1–14. doi: 10.1038/sdata.2016.107.
Haigh, I. D., Ozsoy, O., Wadey, M. P., Nicholls, R. J., Gallop, S. L., Wahl, T., & Brown, J. M. (2017). An improved database of coastal flooding in the United Kingdom from 1915 to 2016. *Scientific Data*, *4*. https://doi.org/10.1038/sdata.2017.100
Hallegatte, S. *et al.* (2013) 'Future flood losses in major coastal cities'. doi: 10.1038/NCLIMATE1979.
Hawkes, P. J. *et al.* (2002) 'The joint probability of waves and water levels in coastal engineering design', *Journal of Hydraulic Research*, 40(3), pp. 241–251. doi: 10.1080/00221680209499940.
Hawkes, P. J. (2005) *Use of Joint Probability Methods in Flood Management: A Guide to Best Practice*, *Flood and Coastal Defence R&D Programme*.
Hawkes, P. and Svensson, C. (2003) *Defra / Environment Agency Flood and Coastal Defence R & D Programme JOINT PROBABILITY : DEPENDENCE MAPPING AND BEST PRACTICE R & D Interim Technical Report Authors :*
Hawkes, P., Svensson, C. and Surendran, S. (2005) 'The joint probability of pairs of variables relevant to fl ood risk: dependence mapping and best practice', *Proceedings of the 40th Defra Flood and Coastal Management Conference*.
Jonkman, S. N. *et al.* (2009) 'Loss of life caused by the flooding of New Orleans after hurricane Katrina: Analysis of the relationship between flood characteristics and mortality', *Risk Analysis*, 29(5), pp. 676–698. doi: 10.1111/j.1539-6924.2008.01190.x.
Kalnay, E. *et al.* (1996) 'The NCEP/NCAR 40-year reanalysis project', *Bulletin of the American Meteorological Society*, pp. 437–471. doi: 10.1175/1520-0477(1996)077<0437:TNYRP>2.0.CO;2.
Kendall, M. G. (1938) 'A New Measure of Rank Correlation', *Biometrika*, 30(1/2), p. 81. doi: 10.2307/2332226.
Kew, S. F. *et al.* (2013) 'The simultaneous occurrence of surge and discharge extremes for the Rhine delta', *Natural Hazards and Earth System Sciences*, 13(8), pp. 2017–2029. doi: 10.5194/nhess-13-2017-2013.
Khanal, S. *et al.* (2018) 'Storm surge and extreme river discharge: a compound event analysis using ensemble impact modelling', *Hydrology and Earth System Sciences Discussions*, (April), pp. 1–25. doi: 10.5194/hess-2018-103.
Kumbier, K. *et al.* (2018) 'Investigating compound flooding in an estuary using hydrodynamic modelling: a case study from the Shoalhaven River, Australia', *Hazards Earth Syst. Sci*, 185194, pp. 463–477. doi: 10.5194/nhess-18-463-2018.
Li, F. *et al.* (2014) 'Probabilistic modelling of extreme storms along the Dutch coast', *Coastal Engineering*, 86, pp. 1–13. doi: 10.1016/j.coastaleng.2013.12.009.
Lian, J. J., Xu, K. and Ma, C. (2013) 'Joint impact of rainfall and tidal level on flood risk in a coastal city with a complex river network: a case study of Fuzhou City, China', *Hydrol. Earth Syst. Sci*, 17, pp. 679–689. doi: 10.5194/hess-17-679-2013.
Marcos, M., Rohmer, J., Vousdoukas, M. I., Mentaschi, L., Le Cozannet, G., & Amores, A. (2019). Increased Extreme Coastal Water Levels Due to the Combined Action of Storm Surges and Wind Waves. *Geophysical Research Letters*, 2019GL082599. https://doi.org/10.1029/2019GL082599

Mantz, P. and Wakeling, H. (1979) 'Forecasting flood levels for joint events of rainfall and tidal surge flooding using extreme ,value statistic', *Proceedings of the Institution of Civil Engineers*. Thomas Telford - ICE Virtual Library, 67(1), pp. 31–50. doi: 10.1680/iicep.1979.2315.

Mazas, F. and Hamm, L. (2017) 'An event-based approach for extreme joint probabilities of waves and sea levels', *Coastal Engineering*. Elsevier, 122(April), pp. 44–59. doi: 10.1016/j.coastaleng.2017.02.003.

McGranahan, G., Balk, D., & Anderson, B. (2007). The rising tide: assessing the risks of climate change and human settlements in low elevation coastal zones. *Environment and Urbanization*, *19*(1), 17–37. https://doi.org/10.1177/0956247807076960

Munich Re. (2017). NatCatSERVICE. Retrieved March 13, 2017, from www.munichre.com/natcatservice.

Neal, R. *et al.* (2016) 'A flexible approach to defining weather patterns and their application in weather forecasting over Europe', *Meteorological Applications*. John Wiley & Sons, Ltd, 23(3), pp. 389–400. doi: 10.1002/met.1563.

Neal, R. *et al.* (2018) 'Use of probabilistic medium- to long-range weather-pattern forecasts for identifying periods with an increased likelihood of coastal flooding around the UK', *Meteorological Applications*, (February), pp. 1–14. doi: 10.1002/met.1719.

Nerem, R.S. *et al.* (2018). Climate-change–driven accelerated sea-level rise detected in the altimeter era. *Proceedings of the National Academy of Sciences*, 115(9), pp.2022-2025.

NOAA (2018) 'Costliest U.S. tropical cyclones tables updated'. doi: 10.1080/00049187308702635.

Orton, P. *et al.* (2015) 'Hazard Assessment from Storm Tides and Rainfall on a Tidal River Estuary', *36th IAHR World Congress*.

Pall, P., Aina, T., Stone, D. A., Stott, P. A., Nozawa, T., Hilberts, A. G. J., … Allen, M. R. (2011). Anthropogenic greenhouse gas contribution to flood risk in England and Wales in autumn 2000. *Nature*, *470*(7334), 382–385. https://doi.org/10.1038/nature09762

Paprotny, D. *et al.* (2018) 'Compound flood potential in Europe', *Hydrology and Earth System Sciences Discussions*, (April), pp. 1–34. doi: 10.5194/hess-2018-132.

Pawlowicz, R., Beardsley, B. and Lentz, A. (2002) 'Classical tidal harmonic analysis including error estimates in MATLAB using T_TIDE', *Computers and Geosciences*, 28, pp. 929–937.

Petroliagkis, T. I. *et al.* (2016) *Joint Probabilities of Storm Surge, Significant Wave Height and River Discharge Components of Coastal Flooding Events. EUR 27824 EN.* doi: doi:10.2788/677778.

Richardson, D. *et al.* (2018) 'A new precipitation and drought climatology based on weather patterns', *International Journal of Climatology*, 38(2), pp. 630–648. doi: 10.1002/joc.5199.

Rueda, A. *et al.* (2016) 'A multivariate extreme wave and storm surge climate emulator based on weather patterns', *Ocean Modelling*, 104, pp. 242–251. doi: 10.1016/j.ocemod.2016.06.008.

Ruocco, A. C. *et al.* (2011) 'Reconstructing coastal flood occurrence combining sea level and media sources: a case study of the Solent, UK since 1935', *Natural Hazards*. Springer Netherlands, 59(3), pp. 1773–1796. doi: 10.1007/s11069-011-9868-7.

Samuels, P. G. and Burt, N. (2002) 'A new joint probability appraisal of flood risk', *Proceedings of the Institution of Civil Engineers: Water and Maritime Engineering*, 154(2), pp. 109–115. doi: 10.1680/maen.154.2.109.38642.

Seneviratne, S. *et al.* (2012) 'Changes in climate extremes and their impacts on the natural physical environment', *Managing the Risk of Extreme Events and Disasters to Advance Climate Change Adaptation.* Cambridge University Press, pp. 109–230. Available at:

https://www.ipcc.ch/pdf/special-reports/srex/SREX-Chap3_FINAL.pdf (Accessed: 21 September 2017).

Svensson, C. and Jones, D. A. (2002) 'Dependence between extreme sea surge, river flow and precipitation in eastern Britain', *International Journal of Climatology*. John Wiley & Sons, Ltd., 22(10), pp. 1149–1168. doi: 10.1002/joc.794.

Svensson, C. and Jones, D. A. (2004) 'Dependence between sea surge, river flow and precipitation in south and west Britain', *Hydrology and Earth System Sciences Discussions European Geosciences Union*, 8(5), pp. 973–992.

Svensson, C. and Jones, D. A. (2005) 'Joint Probability : Dependence between extreme sea surge , river flow and precipitation ':, *R&D Technical Report FD2308/TR3 to DEFRA. CEH Wallingford, Wallingford, UK*.

Thompson, G. and Law, F. (1983) 'An assessment of the fluvial tidal flooding problem of the River Ancholme, UK', in *Proceedings from the IUGG Interdisciplinary Symposium on Assessment of Natural Hazards*. Hamburg.

Wahl, T. *et al.* (2015) 'Increasing risk of compound flooding from storm surge and rainfall for major US cities', *Nature Climate Change*, 5(12), pp. 1093–1097. doi: 10.1038/nclimate2736.

Ward, P. J., Couasnon, A., Eilander, D., Haigh, I. D., Hendry, A., Muis, S., … Wahl, T. (2018). Dependence between high sea-level and high river discharge increases flood hazard in global deltas and estuaries. *Environmental Research Letters*, *13*(8), 084012. https://doi.org/10.1088/1748-9326/aad400

White, C. J. (2007). *The Use of Joint Probability Analysis to Predict Flood Frequency in Estuaries and Tidal Rivers*. University of Southanpton. Retrieved from http://eprints.soton.ac.uk

Wu, W. *et al.* (2018) 'Mapping Dependence Between Extreme Rainfall and Storm Surge', *Journal of Geophysical Research: Oceans*, 123(4), pp. 2461–2474. doi: 10.1002/2017JC013472.

Zheng, F., Westra, S. and Sisson, S. A. (2013) 'Quantifying the dependence between extreme rainfall and storm surge in the coastal zone', *Journal of Hydrology*, 505, pp. 172–187. doi: 10.1016/j.jhydrol.2013.09.054.

Zscheischler, J. *et al.* (2018) 'Future climate risk from compound events', *Nature Climate Change*. Nature Publishing Group, p. 1. doi: 10.1038/s41558-018-0156-3.

Figures

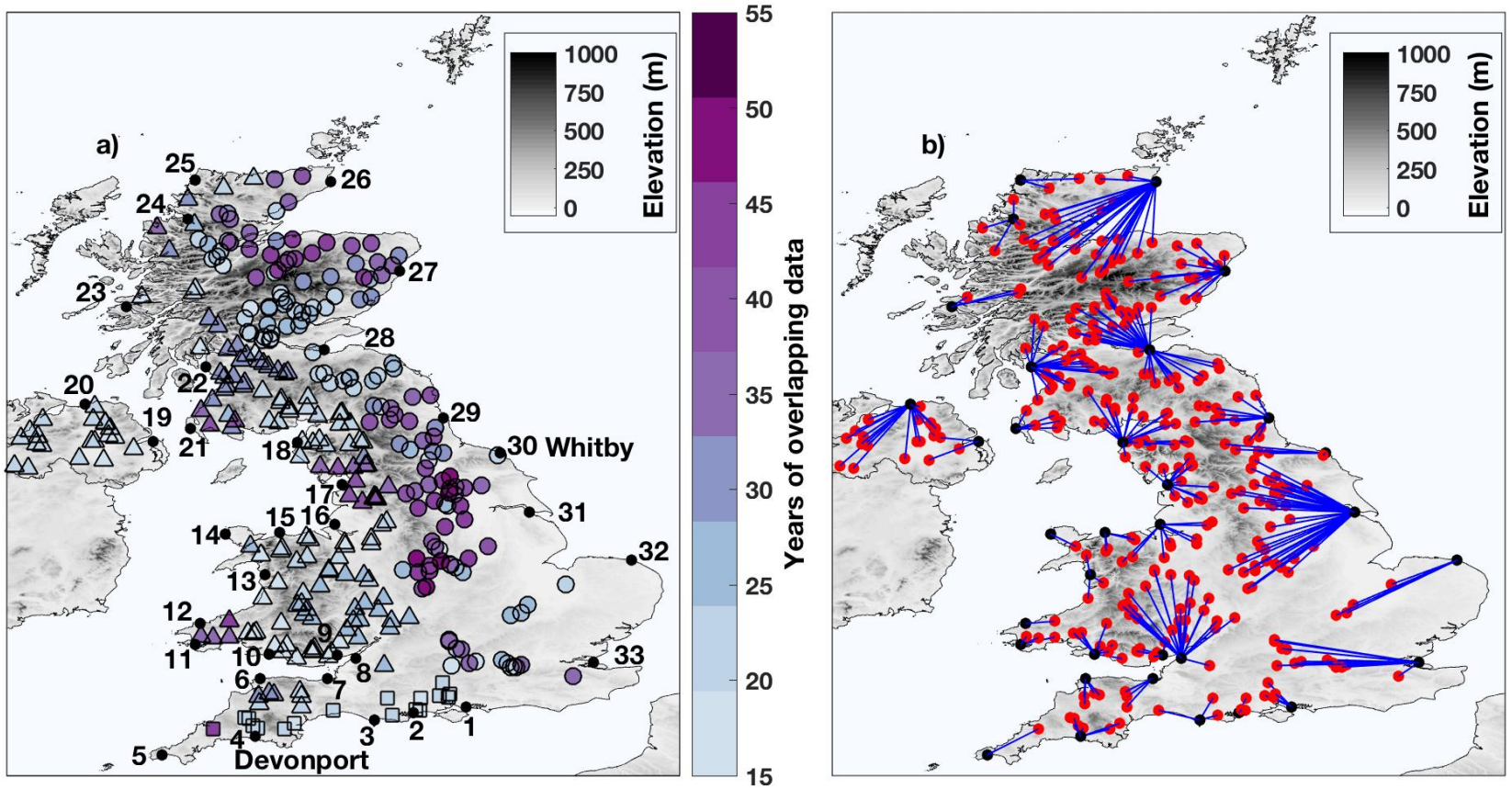

Figure 1: (a) Location and overlapping data length (in years) of the 33 tide gauge sites (black dots) and 326 river discharge stations (triangles, circles and squares show the river stations that discharge onto the west, east and south coasts, respectively); and (b) pairing of the tide gauge and river discharge stations.

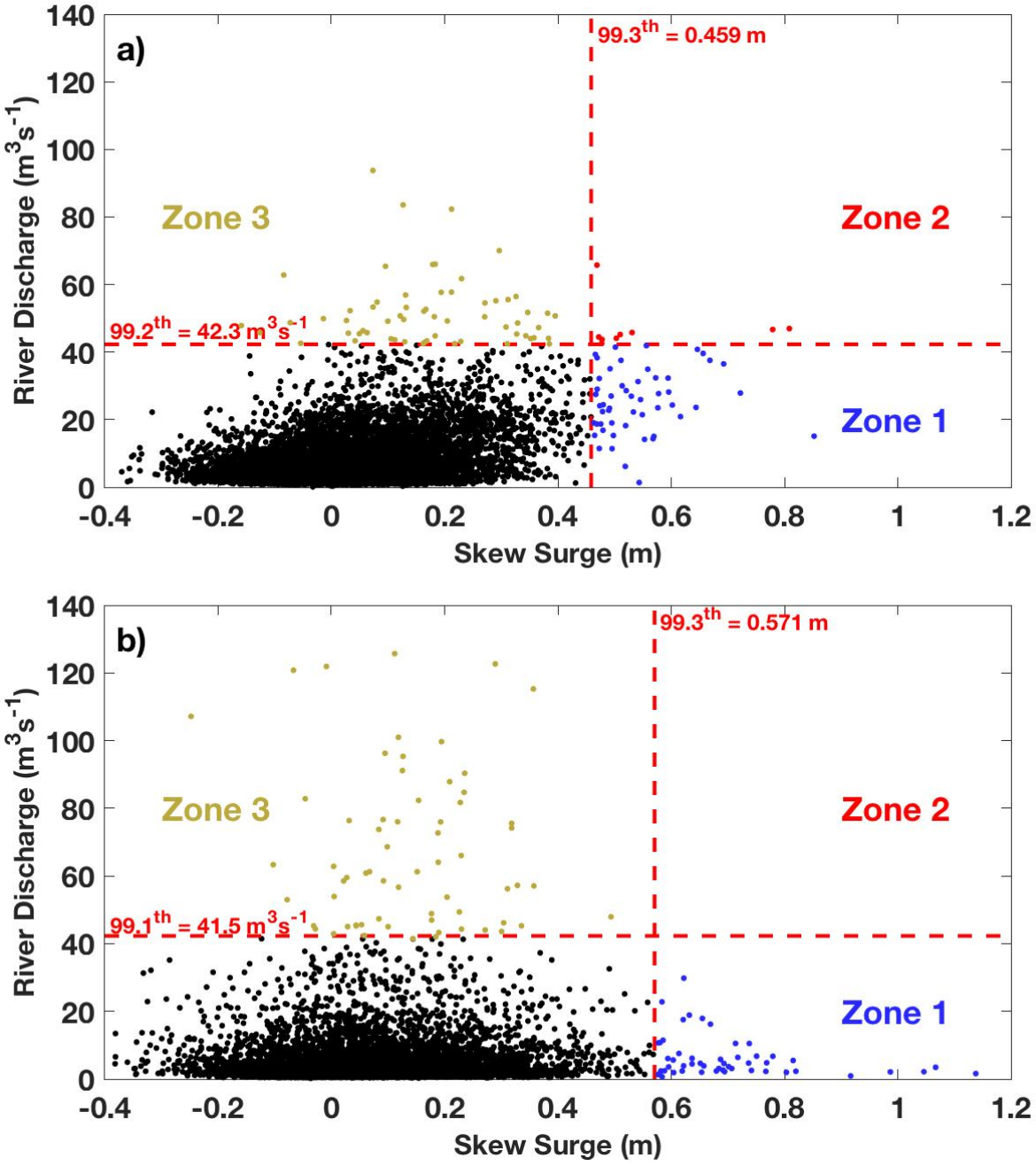

Figure 2: Daily maximum skew surge plotted against daily maximum river discharge for (a) Devonport; and (b) Whitby. The dotted red lines indicate the high percentiles chosen in the analysis for the two variables at these sites. Red dots (plotted in Zone 2) show the events with potential for compound flooding (i.e., joint occurrence of high storm surge and large river discharge) whereas blue (Zone 1) and green (Zone 3) define the non-compound events (i.e., high storm surge or high river discharge only, respectively).

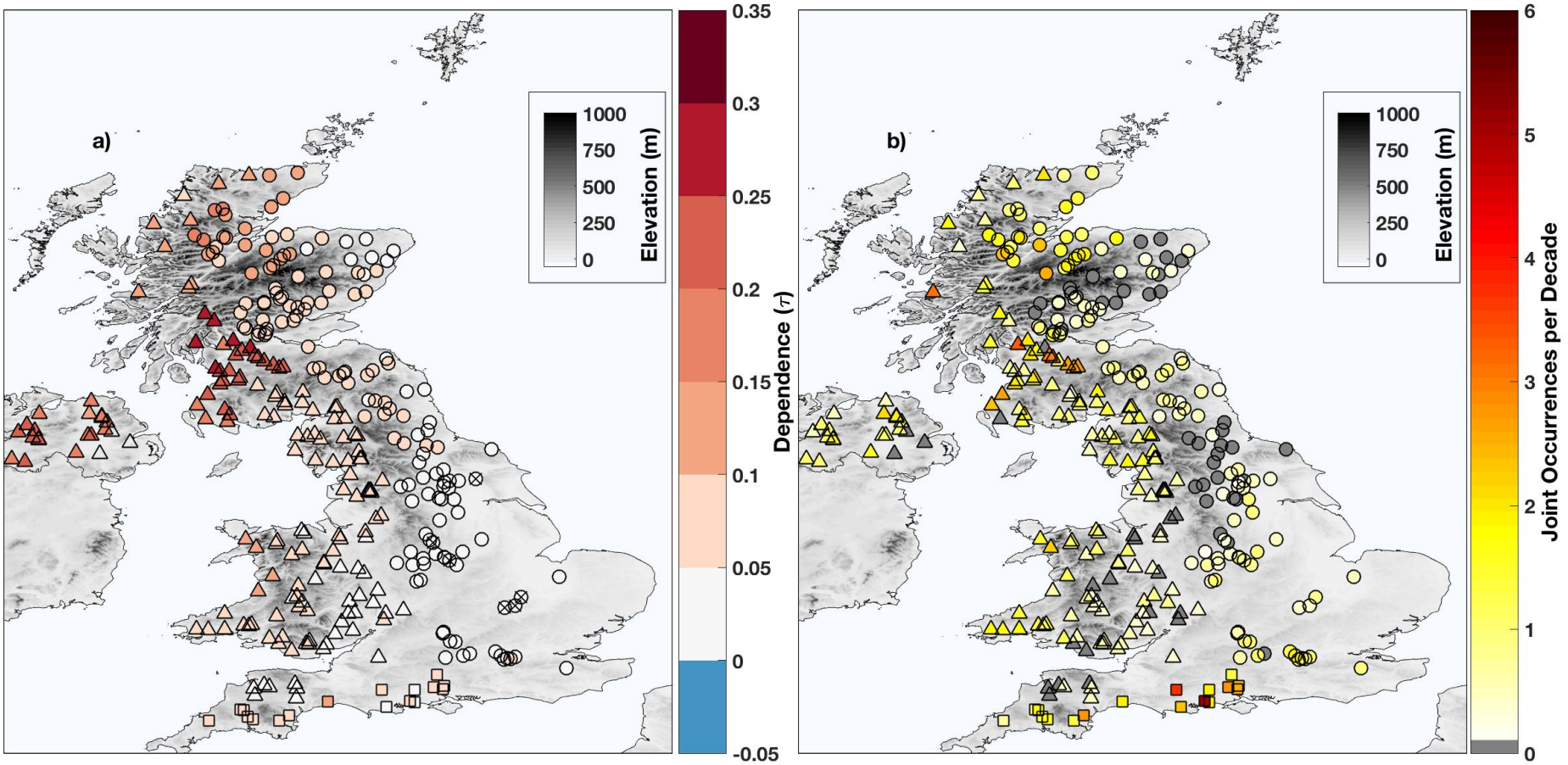

Figure 3: (a) Kendall's Rank Correlation τ between daily maximum total sea level and daily maximum river discharge; and (b) number of joint occurrences per decade between extreme total sea levels and river discharge, at 0-day lag. Thick black lines in (a) represent that the dependence is statistically significant (95% confidence) at these sites. Note that the triangles, circles and squares show the river stations that discharge onto the west, east and south coasts, respectively.

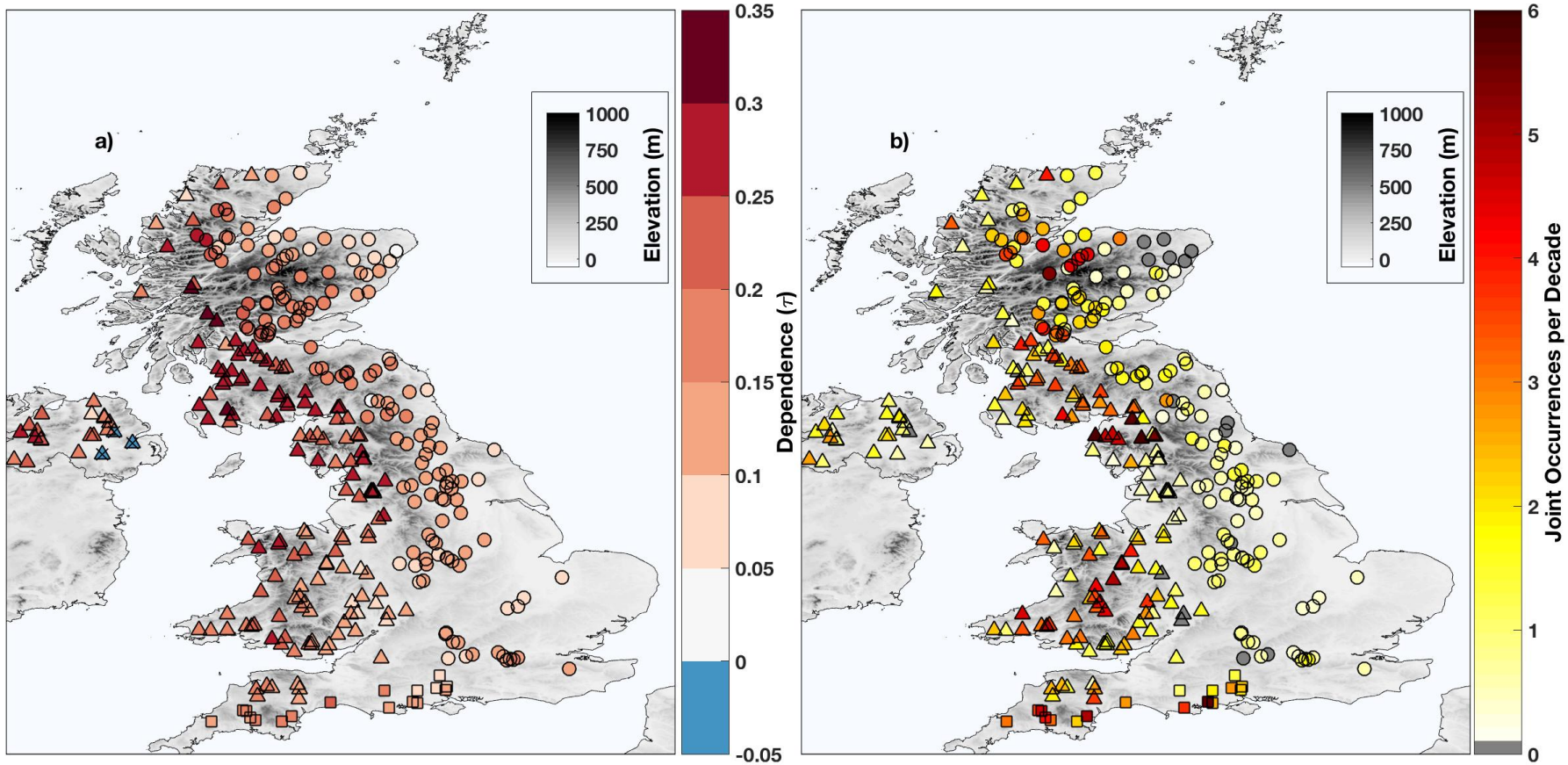

Figure 4: (a) Kendall's Rank Correlation τ between daily maximum skew surge and daily maximum river discharge; and (b) number of joint occurrences per decade between extreme skew surge and extreme river discharge, at 0-day lag. Sites with across through them in (a) represent that the dependence is not statistically significant (95% confidence) at these sites. Note that the triangles, circles and squares show the river stations that discharge onto the west, east and south coasts, respectively.

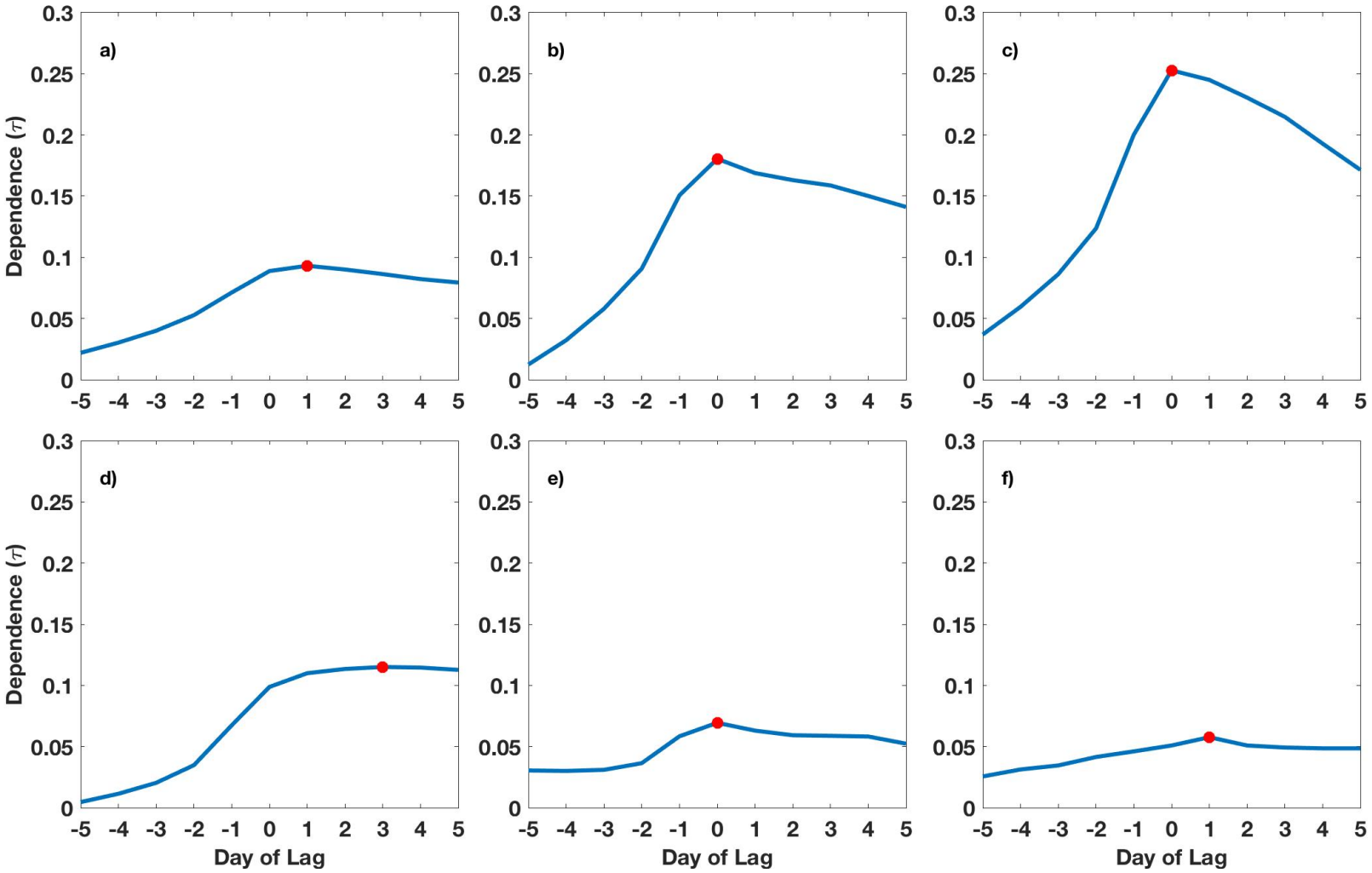

Figure 5: Kendall's Rank Correlation τ plotted against day of lag at the follow sites: (a) Bournemouth [2]; (b) Devonport [5]; (c) Workington [18]; (d) Ullapool [24]; (e) Whitby [30]; and (f) Cromer [32]. The red dot shows the day with maximum lag.

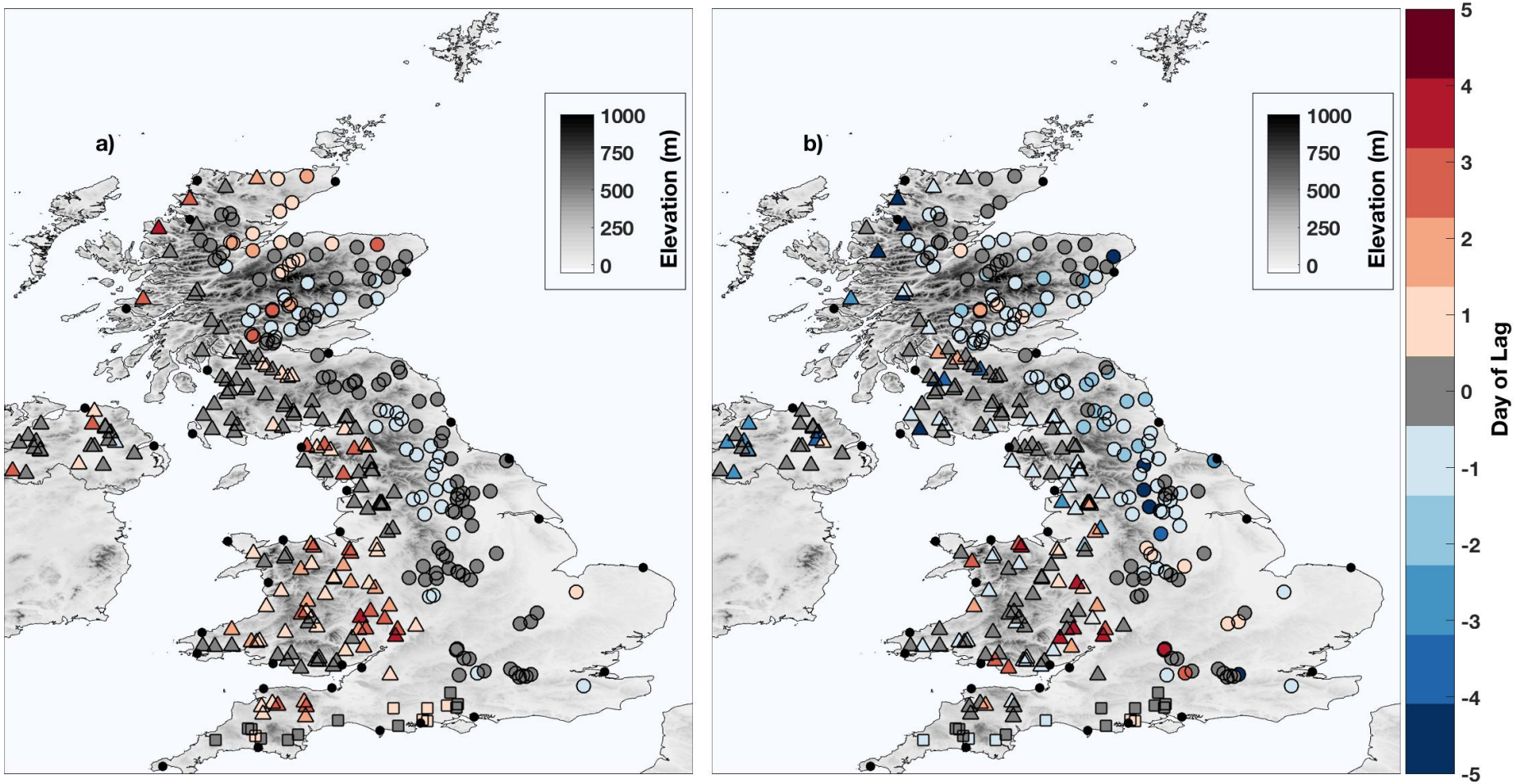

Figure 6: (a) The lag day when the Kendall's Rank Correlation τ is maximum between daily maximum skew surge and daily maximum river discharge; and (b) when the lag day when the number of joint occurrences between high skew surge and high river discharge is maximum. Note that the triangles, circles and squares show the river stations that discharge onto the west, east and south coasts, respectively.

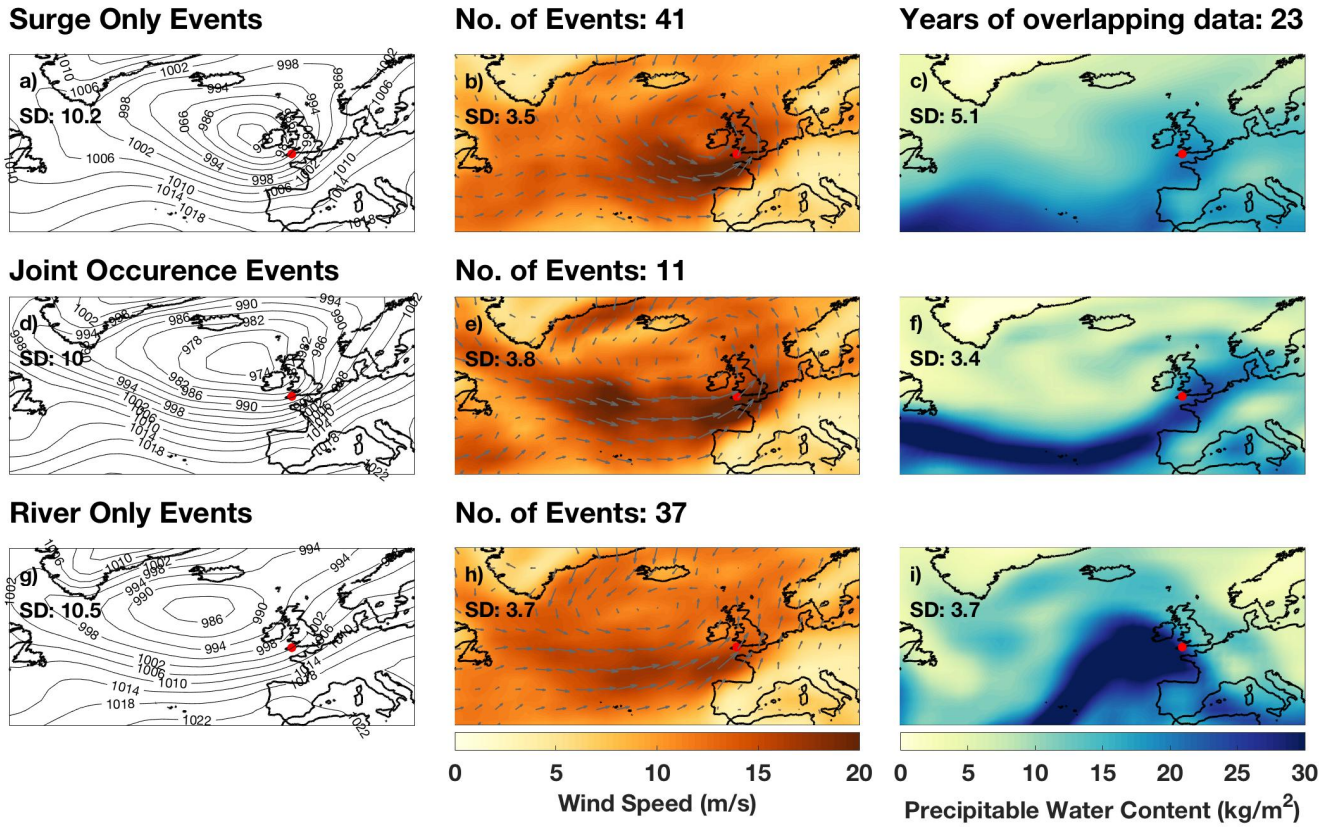

Figure 7: Meteorology conditions for Devonport [5]: first column, sea level pressure (mbar); second column, wind speed (m/s) and direction (grey arrows); third column, precipitable water content (kg/m^2); during (a, b and c) high skew surge events only, (d, e and f) both high skew surge and high river discharge events, and (g, h and i) extreme high river discharge events only. SD correspond to the averaged standard deviation over the grid for each variable across the selected events.

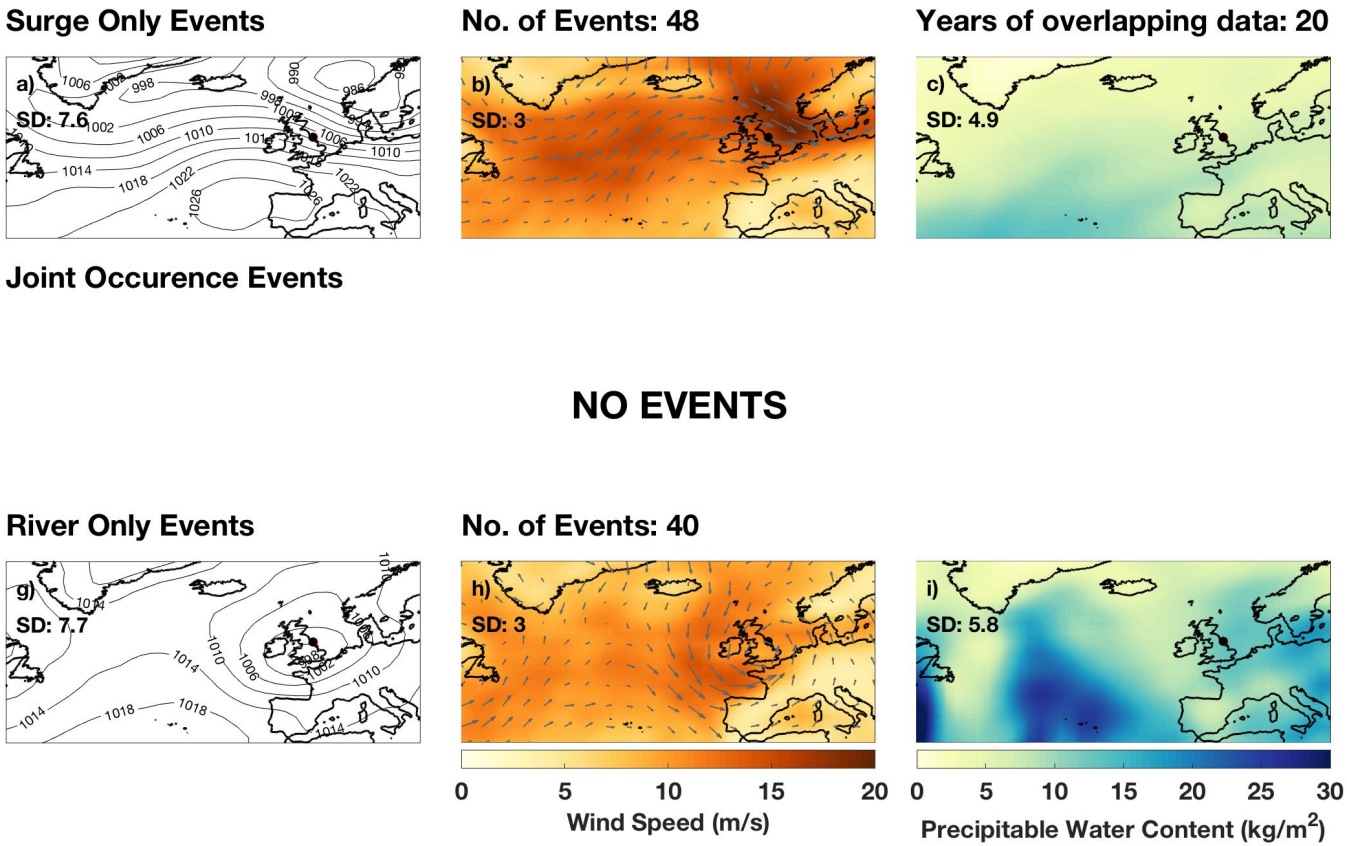

Figure 8: Meteorology conditions for Whitby [30]: first column, sea level pressure (mbar); second column, wind speed (m/s) and direction (grey arrows); third column, precipitable water content (kg/m^2); during (a, b and c) high skew surge only events, (d, e and f) both high skew surge and high river discharge events, and (g, h and i) extreme high river discharge only events. SD correspond to the averaged standard deviation over the grid for each variable across the selected events.

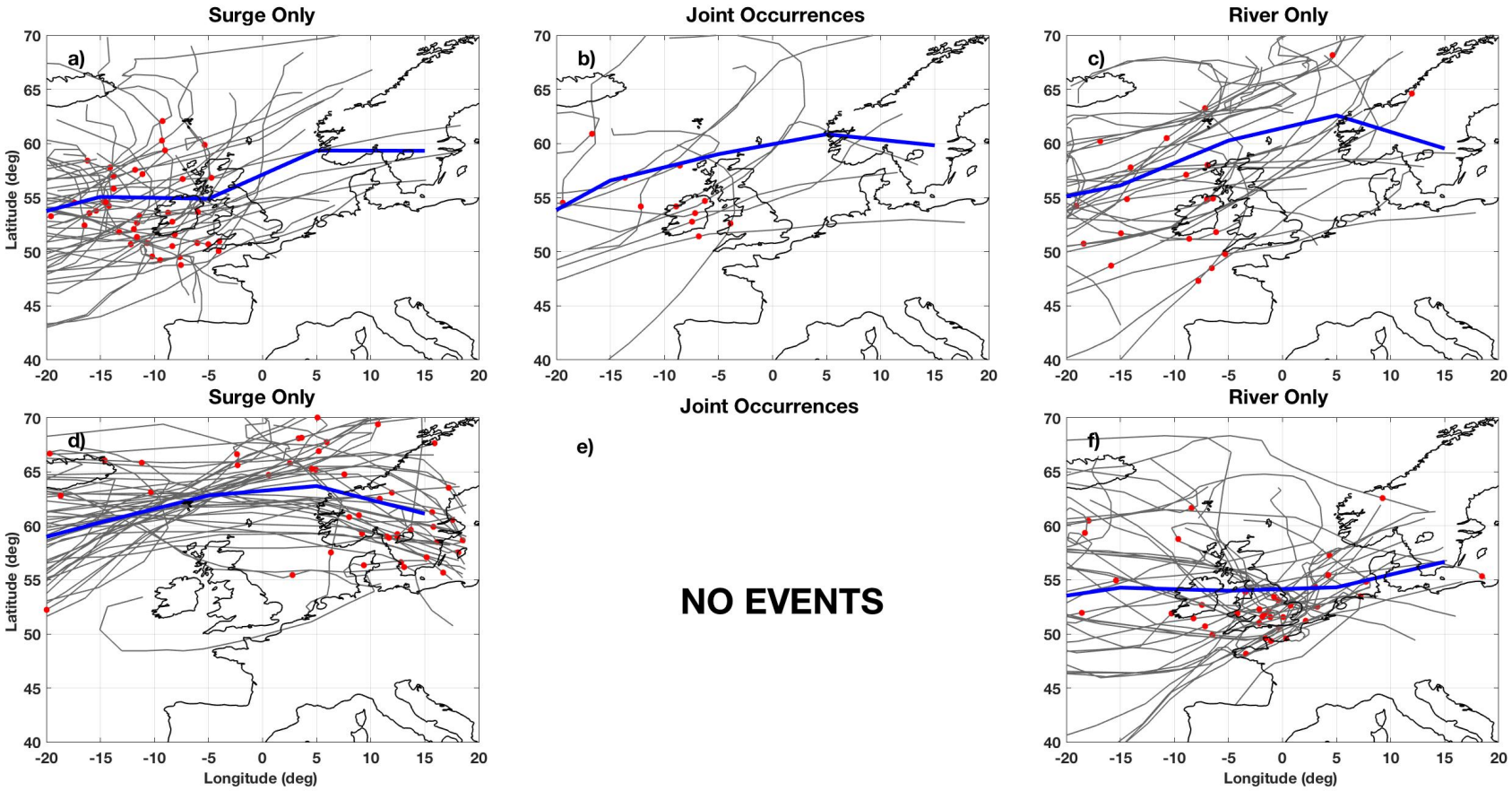

Figure 9: Storm tracks for Devonport [5] (a, b and c) and Whitby [30] (d, e and f) over Northern Europe. The first column (a, d) shows high skew surge only events. The second column (b, e) both high skew surge and high river discharge events. The third column (c, f) shows high river discharge only events. The blue line represents the mean storm track. Grey lines show individual storm tracks with the location of the storm at peak skew surge and/or peak river discharge shown by the red dot.

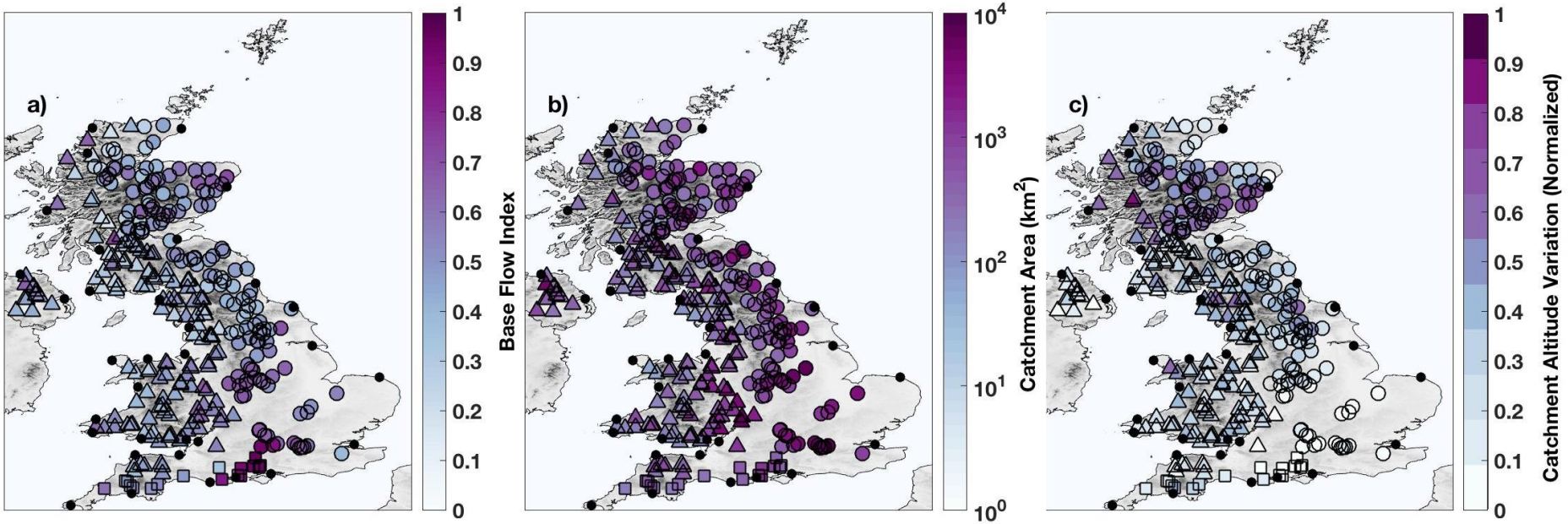

Figure 10: (a) Base flow index; (b) catchment area size (logged km^2); and (c) catchment altitude variation (normalised). Note that the triangles, circles and squares show the river stations that discharge onto the west, east and south coasts, respectively.

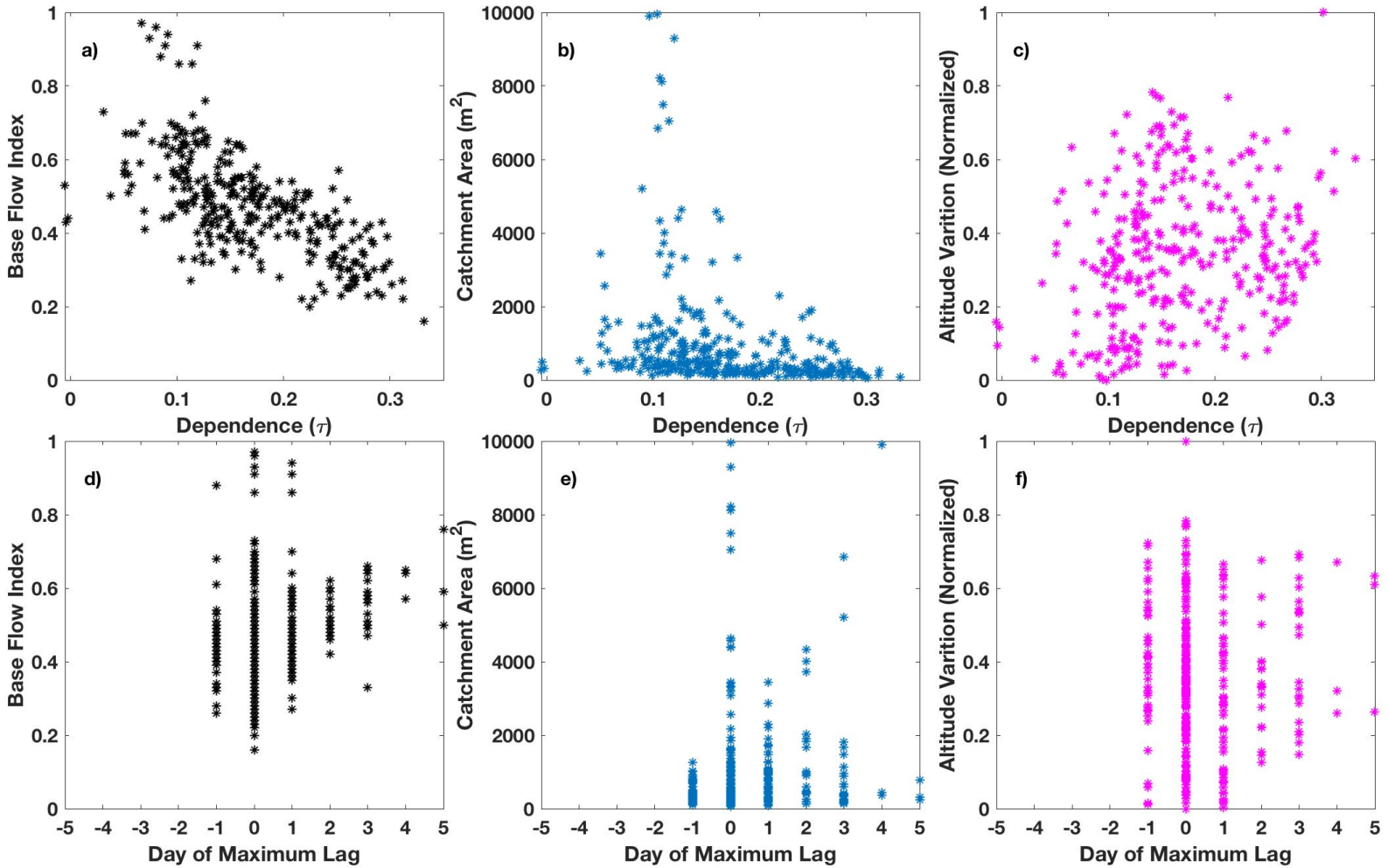

Figure 11: Kendall's Rank Correlation τ between daily maximum skew surge and daily maximum river discharge with: (a) base flow index; (b) catchment area size (logged km^2); (c) catchment altitude variation (normalised); and correlation of the day of lag with the largest Kendall's Rank Correlation τ with: (d) base flow index; (e) catchment area size (logged km^2); (f) catchment altitude variation (normalised), for all sites.

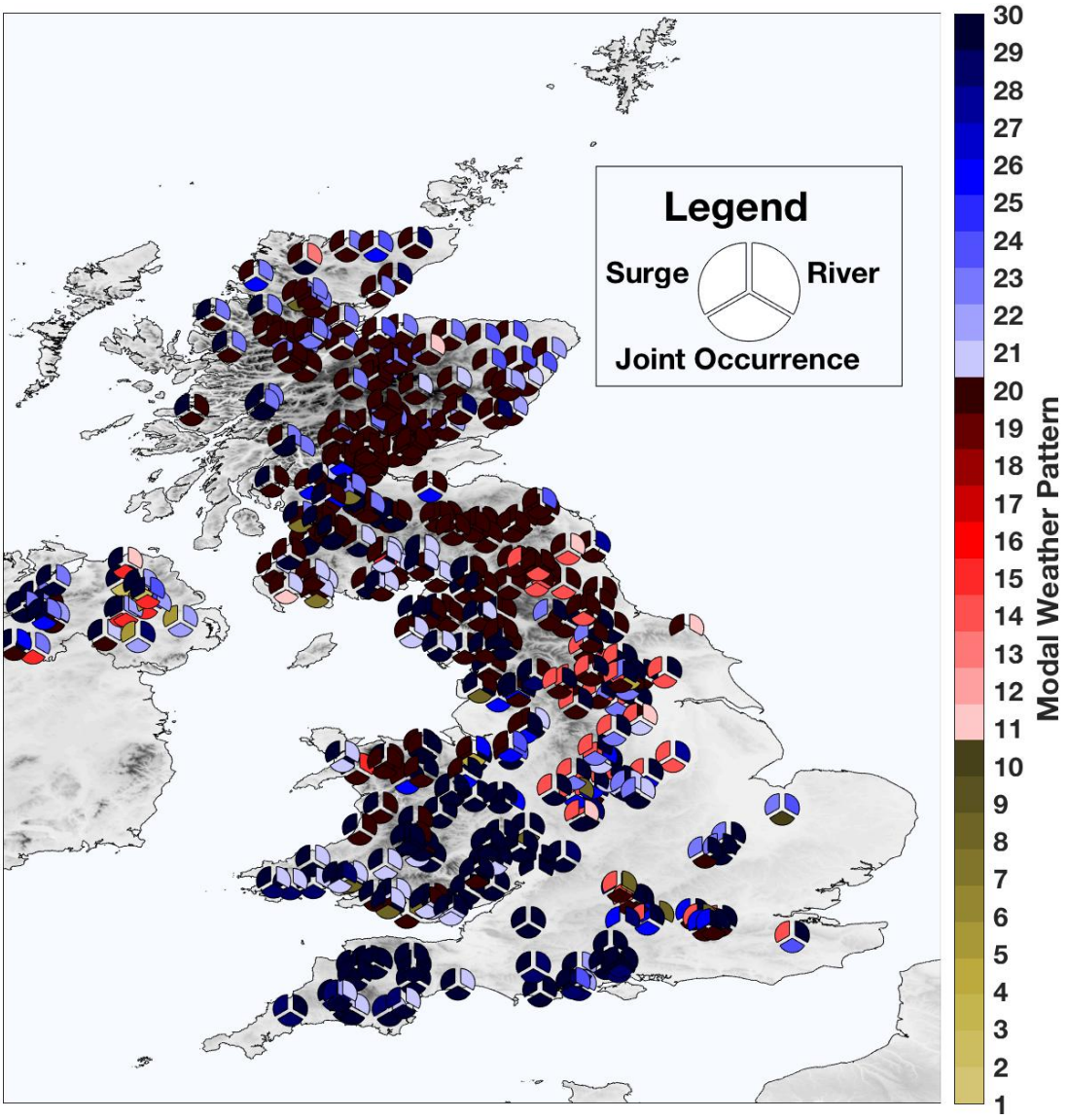

Figure 12: The modal weather pattern type (indicated by the colours in the legend) for extreme surge only events (top left segment), extreme river flow only events (top right segment), and extreme joint occurrence events (bottom segment) observed at the study locations.

Tables

Table 1: The pairs of tide gauge sites and river discharge stations used in the study.

Tide Gauge	Tide Gauge Latitude (deg)	Tide Gauge longitude (deg)	River Gauge ID	River	River Gauge Location	River Gauge Latitude (deg)	River Gauge longitude (deg)
Aberdeen	57.14	-2.08	12002	Dee	Park	57.08	-2.33
Aberdeen	57.14	-2.08	12001	Dee	Woodend	57.05	-2.60
Aberdeen	57.14	-2.08	12003	Dee	Polhollick	57.06	-3.08
Aberdeen	57.14	-2.08	11001	Don	Parkhill	57.22	-2.19
Aberdeen	57.14	-2.08	13007	North Esk	Logie Mill	56.77	-2.49
Aberdeen	57.14	-2.08	9002	Deveron	Muiresk	57.54	-2.49
Aberdeen	57.14	-2.08	11002	Don	Haughton	57.27	-2.40
Aberdeen	57.14	-2.08	13008	South Esk	Brechin	56.73	-2.65
Aberdeen	57.14	-2.08	12007	Dee	Mar Lodge	56.99	-3.49
Aberdeen	57.14	-2.08	11003	Don	Bridge of Alford	57.24	-2.72
Aberdeen	57.14	-2.08	9001	Deveron	Avochie	57.51	-2.78
Aberdeen	57.14	-2.08	10003	Ythan	Ellon	57.36	-2.09
Aberdeen	57.14	-2.08	12008	Feugh	Heugh Head	57.03	-2.52
Aberdeen	57.14	-2.08	13012	South Esk	Gella Bridge	56.78	-3.03
Avonmouth	51.51	-2.71	54057	Severn	Haw Bridge	51.95	-2.23
Avonmouth	51.51	-2.71	54032	Severn	Saxons Lode	52.05	-2.20
Avonmouth	51.51	-2.71	55023	Wye	Redbrook	51.80	-2.69
Avonmouth	51.51	-2.71	54001	Severn	Bewdley	52.38	-2.32
Avonmouth	51.51	-2.71	54095	Severn	Buildwas	52.64	-2.52
Avonmouth	51.51	-2.71	55002	Wye	Belmont	52.04	-2.75
Avonmouth	51.51	-2.71	54005	Severn	Montford	52.72	-2.87
Avonmouth	51.51	-2.71	55007	Wye	Erwood	52.09	-3.35
Avonmouth	51.51	-2.71	54028	Vyrnwy	Llanymynech	52.77	-3.11
Avonmouth	51.51	-2.71	53018	Avon	Bathford	51.40	-2.31

Avonmouth	51.51	-2.71	54029	Teme	Knightsford Bridge	52.20	-2.39
Avonmouth	51.51	-2.71	54002	Avon	Evesham	52.09	-1.94
Avonmouth	51.51	-2.71	54014	Severn	Abermule	52.55	-3.23
Avonmouth	51.51	-2.71	54008	Teme	Tenbury	52.31	-2.59
Avonmouth	51.51	-2.71	55003	Lugg	Lugwardine	52.06	-2.66
Avonmouth	51.51	-2.71	55012	Irfon	Cilmery	52.15	-3.47
Avonmouth	51.51	-2.71	55016	Ithon	Disserth	52.21	-3.43
Avonmouth	51.51	-2.71	54080	Severn	Dolwen	52.45	-3.49
Avonmouth	51.51	-2.71	54012	Tern	Walcot	52.71	-2.60
Avonmouth	51.51	-2.71	54038	Tanat	Llanyblodwel	52.79	-3.11
Avonmouth	51.51	-2.71	55026	Wye	Ddol Farm	52.30	-3.50
Avonmouth	51.51	-2.71	55029	Monnow	Grosmont	51.92	-2.85
Avonmouth	51.51	-2.71	55021	Lugg	Butts Bridge	52.23	-2.73
Avonmouth	51.51	-2.71	55032	Elan	Caban Dam	52.27	-3.57
Bangor	54.66	-5.67	205004	Lagan	Newforge	54.55	-5.95
Bangor	54.66	-5.67	203018	Six-Mile Water	Antrim	54.72	-6.22
Bangor	54.66	-5.67	203097	Upper Bann	Moyallen	54.39	-6.39
Barmouth	52.72	-4.05	64001	Dyfi	Dyfi Bridge	52.60	-3.85
Barmouth	52.72	-4.05	63001	Ystwyth	Pont Llolwyn	52.38	-4.07
Barmouth	52.72	-4.05	65001	Glaslyn	Beddgelert	53.01	-4.10
Bournemouth	50.71	-1.87	43021	Avon	Knapp Mill	50.75	-1.78
Bournemouth	50.71	-1.87	43003	Avon	East Mills Total	50.93	-1.77
Bournemouth	50.71	-1.87	43007	Stour	Throop	50.76	-1.84
Cromer	52.93	1.30	33035	Ely Ouse	Denver Complex	52.58	0.35
Cromer	52.93	1.30	33026	Bedford Ouse	Offord	52.29	-0.22
Cromer	52.93	1.30	33039	Bedford Ouse	Roxton	52.17	-0.30

Cromer	52.93	1.30	33002	Bedford Ouse	Bedford	52.13	-0.46
Devonport	50.37	-4.19	47001	Tamar	Gunnislake	50.53	-4.22
Devonport	50.37	-4.19	46003	Dart	Austins Bridge	50.48	-3.76
Devonport	50.37	-4.19	47019	Tamar	Polson Bridge	50.64	-4.33
Devonport	50.37	-4.19	46002	Teign	Preston	50.56	-3.62
Devonport	50.37	-4.19	47015	Tavy	Ludbrook	50.49	-4.15
Devonport	50.37	-4.19	47006	Lyd	Lifton Park	50.64	-4.28
Fishguard	52.01	-4.98	62001	Teifi	Glanteifi	52.05	-4.56
Heysham	54.03	-2.92	72004	Lune	Caton	54.08	-2.72
Heysham	54.03	-2.92	71001	Ribble	Samlesbury	53.77	-2.62
Heysham	54.03	-2.92	71009	Ribble	New Jumbles Rock	53.83	-2.45
Heysham	54.03	-2.92	73010	Leven	Newby Bridge	54.27	-2.97
Heysham	54.03	-2.92	71006	Ribble	Henthorn	53.85	-2.42
Heysham	54.03	-2.92	72005	Lune	Killington	54.31	-2.58
Heysham	54.03	-2.92	73005	Kent	Sedgwick	54.28	-2.75
Heysham	54.03	-2.92	72011	Rawthey	Brigflatts	54.31	-2.55
Heysham	54.03	-2.92	71008	Hodder	Hodder Place	53.85	-2.45
Heysham	54.03	-2.92	71004	Calder	Whalley Weir	53.82	-2.41
Heysham	54.03	-2.92	71011	Ribble	Arnford	54.00	-2.25
Heysham	54.03	-2.92	72002	Wyre	St Michaels	53.86	-2.82
Heysham	54.03	-2.92	72015	Lune	Lunes Bridge	54.42	-2.60
Heysham	54.03	-2.92	74001	Duddon	Duddon Hall	54.30	-3.24
Hinkley	51.22	-3.13	45001	Exe	Thorverton	50.80	-3.51
Hinkley	51.22	-3.13	45002	Exe	Stoodleigh	50.95	-3.51
Hinkley	51.22	-3.13	45011	Barle	Brushford	51.02	-3.53
Holyhead	53.31	-4.62	65006	Seiont	Peblig Mill	53.14	-4.25
Ilfracombe	51.21	-4.11	50001	Taw	Umberleigh	50.99	-3.99
Ilfracombe	51.21	-4.11	50002	Torridge	Torrington	50.95	-4.14

Ilfracombe	51.21	-4.11	50006	Mole	Woodleigh	50.97	-3.91
Ilfracombe	51.21	-4.11	50010	Torridge	Rockhay Bridge	50.84	-4.12
Immingham	53.63	-0.19	28022	Trent	North Muskham	53.14	-0.80
Immingham	53.63	-0.19	28009	Trent	Colwick	52.95	-1.08
Immingham	53.63	-0.19	28007	Trent	Shardlow	52.86	-1.33
Immingham	53.63	-0.19	27009	Ouse	Skelton	53.99	-1.13
Immingham	53.63	-0.19	28019	Trent	Drakelow Park	52.78	-1.65
Immingham	53.63	-0.19	27003	Aire	Beal Weir	53.72	-1.20
Immingham	53.63	-0.19	27007	Ure	Westwick Lock	54.10	-1.46
Immingham	53.63	-0.19	27071	Swale	Crakehill	54.15	-1.35
Immingham	53.63	-0.19	27079	Calder	Methley	53.73	-1.38
Immingham	53.63	-0.19	28067	Derwent	Church Wilne	52.88	-1.34
Immingham	53.63	-0.19	27080	Aire	Lemonroyd	53.75	-1.42
Immingham	53.63	-0.19	27002	Wharfe	Flint Mill Weir	53.92	-1.36
Immingham	53.63	-0.19	27089	Wharfe	Tadcaster	53.89	-1.27
Immingham	53.63	-0.19	28085	Derwent	St Mary's Bridge	52.93	-1.47
Immingham	53.63	-0.19	27041	Derwent	Buttercrambe	54.02	-0.88
Immingham	53.63	-0.19	27034	Derwent	Stamford Bridge	54.27	-1.71
Immingham	53.63	-0.19	27021	Don	Doncaster	53.53	-1.14
Immingham	53.63	-0.19	27028	Aire	Armley	53.80	-1.57
Immingham	53.63	-0.19	28117	Derwent	Whatstandwell	53.09	-1.51
Immingham	53.63	-0.19	27043	Wharfe	Addingham	53.94	-1.86
Immingham	53.63	-0.19	28080	Tame	Lea Marston Lakes	52.54	-1.69
Immingham	53.63	-0.19	28018	Dove	Marston on Dove	52.86	-1.65
Immingham	53.63	-0.19	27090	Swale	Catterick Bridge	54.39	-1.65

Immingham	53.63	-0.19	28011	Derwent	Matlock Bath	53.12	-1.56
Immingham	53.63	-0.19	28012	Trent	Yoxall	52.76	-1.80
Immingham	53.63	-0.19	28074	Soar	Kegworth	52.83	-1.27
Immingham	53.63	-0.19	28093	Soar	Pillings Lock	52.76	-1.16
Immingham	53.63	-0.19	27062	Nidd	Skip Bridge	54.00	-1.26
Immingham	53.63	-0.19	27029	Calder	Elland	53.69	-1.81
Immingham	53.63	-0.19	27001	Nidd	Hunsingore Weir	53.97	-1.35
Immingham	53.63	-0.19	28008	Dove	Rocester Weir	52.95	-1.83
Immingham	53.63	-0.19	27035	Aire	Kildwick Bridge	53.91	-1.98
Immingham	53.63	-0.19	28043	Derwent	Chatsworth	53.21	-1.61
Immingham	53.63	-0.19	28014	Sow	Milford	52.79	-2.04
Immingham	53.63	-0.19	28003	Tame	Water Orton	52.52	-1.75
Immingham	53.63	-0.19	27006	Don	Hadfields Weir	53.41	-1.41
Immingham	53.63	-0.19	27053	Nidd	Birstwith	54.04	-1.65
Kinlochbervie	58.46	-5.05	96002	Naver	Apigill	58.48	-4.21
Kinlochbervie	58.46	-5.05	96004	Strathmore	Allnabad	58.35	-4.65
Leith	55.99	-3.18	15006	Tay	Ballathie	56.51	-3.39
Leith	55.99	-3.18	15003	Tay	Caputh	56.54	-3.49
Leith	55.99	-3.18	21009	Tweed	Norham	55.72	-2.16
Leith	55.99	-3.18	15012	Tummel	Pitlochry	56.70	-3.72
Leith	55.99	-3.18	21021	Tweed	Sprouston	55.61	-2.39
Leith	55.99	-3.18	15007	Tay	Pitnacree	56.66	-3.76
Leith	55.99	-3.18	15016	Tay	Kenmore	56.60	-3.99
Leith	55.99	-3.18	18011	Forth	Craigforth	56.14	-3.97
leith	55.99	-3.18	21006	Tweed	Boleside	55.59	-2.80
Leith	55.99	-3.18	16004	Earn	Forteviot Bridge	56.35	-3.55
Leith	55.99	-3.18	18003	Teith	Bridge of Teith	56.19	-4.06

Leith	55.99	-3.18	16001	Earn	Kinkell Bridge	56.33	-3.73
Leith	55.99	-3.18	21008	Teviot	Ormiston Mill	55.55	-2.47
Leith	55.99	-3.18	15034	Garry	Killiecrankie	56.75	-3.80
Leith	55.99	-3.18	21003	Tweed	Peebles	55.65	-3.18
Leith	55.99	-3.18	15024	Dochart	Killin	56.46	-4.33
Leith	55.99	-3.18	18010	Forth	Gargunnock	56.13	-4.07
Leith	55.99	-3.18	21007	Ettrick Water	Lindean	55.57	-2.82
Leith	55.99	-3.18	15025	Ericht	Craighall	56.61	-3.35
Leith	55.99	-3.18	18008	Leny	Anie	56.26	-4.29
Leith	55.99	-3.18	15011	Lyon	Comrie Bridge	56.61	-3.98
Leith	55.99	-3.18	21005	Tweed	Lyne Ford	55.64	-3.26
Leith	55.99	-3.18	21012	Teviot	Hawick	55.43	-2.76
Leith	55.99	-3.18	15010	Isla	Wester Cardean	56.61	-3.15
Leith	55.99	-3.18	18015	Eas Gobhain	Loch Venachar	56.23	-4.26
Leith	55.99	-3.18	15039	Tilt	Marble Lodge	56.82	-3.82
Leith	55.99	-3.18	15023	Braan	Hermitage	56.56	-3.61
Leith	55.99	-3.18	18005	Allan Water	Bridge of Allan	56.16	-3.96
Leith	55.99	-3.18	15041	Lyon	Camusvrachan	56.60	-4.25
Leith	55.99	-3.18	21022	Whiteadder Water	Hutton Castle	55.79	-2.19
Leith	55.99	-3.18	21011	Yarrow Water	Philiphaugh	55.54	-2.89
Leith	55.99	-3.18	19001	Almond	Craigiehall	55.96	-3.34
Leith	55.99	-3.18	15013	Almond	Almondbank	56.42	-3.51
Leith	55.99	-3.18	18001	Allan Water	Kinbuck	56.23	-3.95

Leith	55.99	-3.18	16003	Ruchill Water	Cultybraggan	56.36	-4.00
Leith	55.99	-3.18	21020	Yarrow Water	Gordon Arms	55.51	-3.09
Liverpool	53.45	-3.02	67027	Dee	Ironbridge	53.13	-2.87
Liverpool	53.45	-3.02	67033	Dee	Chester Suspension Bridge	53.19	-2.88
Liverpool	53.45	-3.02	67015	Dee	Manley Hall	52.97	-2.97
Liverpool	53.45	-3.02	69002	Irwell	Adelphi Weir	53.49	-2.26
Liverpool	53.45	-3.02	67001	Dee	Bala	52.91	-3.58
Liverpool	53.45	-3.02	69007	Mersey	Ashton Weir	53.44	-2.34
Liverpool	53.45	-3.02	68001	Weaver	Ashbrook	53.17	-2.49
Liverpool	53.45	-3.02	67006	Alwen	Druid	52.98	-3.43
Liverpool	53.45	-3.02	68003	Dane	Rudheath	53.24	-2.50
Llandudno	53.33	-3.83	66011	Conwy	Cwmlanerch	53.11	-3.79
Llandudno	53.33	-3.83	66025	Clwyd	Pont Dafydd	53.26	-3.43
Llandudno	53.33	-3.83	66001	Clwyd	Pont-y-Cambwll	53.23	-3.39
Llandudno	53.33	-3.83	66012	Lledr	Pont Gethin	53.07	-3.81
Milford Haven	51.71	-5.05	60003	Taf	Clog-y-Fran	51.81	-4.56
Milford Haven	51.71	-5.05	61002	Eastern Cleddau	Canaston Bridge	51.80	-4.80
Milford Haven	51.71	-5.05	61001	Western Cleddau	Prendergast Mill	51.82	-4.97
Millport	55.75	-4.91	84013	Clyde	Daldowie	55.83	-4.12
Millport	55.75	-4.91	85001	Leven	Linnbrane	55.99	-4.58
Millport	55.75	-4.91	84005	Clyde	Blairston	55.80	-4.07
Millport	55.75	-4.91	84003	Clyde	Hazelbank	55.69	-3.85
Millport	55.75	-4.91	84018	Clyde	Tulliford Mill	55.64	-3.76
Millport	55.75	-4.91	89003	Orchy	Glen Orchy	56.45	-4.86

Millport	55.75	-4.91	84004	Clyde	Sills of Clyde	55.66	-3.70
Millport	55.75	-4.91	83006	Ayr	Mainholm	55.46	-4.59
Millport	55.75	-4.91	86002	Eachaig	Eckford	56.02	-4.99
Millport	55.75	-4.91	83005	Irvine	Shewalton	55.60	-4.63
Millport	55.75	-4.91	84001	Kelvin	Killermont	55.91	-4.31
Millport	55.75	-4.91	84014	Avon Water	Fairholm	55.74	-3.99
Millport	55.75	-4.91	85002	Endrick Water	Gaidrew	56.05	-4.44
Millport	55.75	-4.91	82002	Doon	Auchendrane	55.41	-4.63
Millport	55.75	-4.91	84015	Kelvin	Dryfield	55.94	-4.18
Millport	55.75	-4.91	82001	Girvan	Robstone	55.26	-4.81
Millport	55.75	-4.91	84012	White Cart Water	Hawkhead	55.84	-4.40
Millport	55.75	-4.91	83009	Garnock	Kilwinning	55.65	-4.69
Millport	55.75	-4.91	83013	Irvine	Glenfield	55.60	-4.49
Millport	55.75	-4.91	85003	Falloch	Glen Falloch	56.34	-4.72
Millport	55.75	-4.91	83004	Lugar Water	Langholm	55.47	-4.36
Millport	55.75	-4.91	83003	Ayr	Catrine	55.50	-4.34
Mumbles	51.57	-3.98	60010	Tywi	Capel Dewi	51.86	-4.20
Mumbles	51.57	-3.98	59001	Tawe	Ynystanglws	51.68	-3.90
Mumbles	51.57	-3.98	60002	Cothi	Felin Mynachdy	51.88	-4.17
Mumbles	51.57	-3.98	60007	Tywi	Dolau Hirion	52.01	-3.81
Mumbles	51.57	-3.98	58002	Neath	Resolven	51.70	-3.72
Mumbles	51.57	-3.98	58001	Ogmore	Bridgend	51.50	-3.58
Mumbles	51.57	-3.98	58012	Afan	Marcroft Weir	51.60	-3.78
Mumbles	51.57	-3.98	60006	Gwili	Glangwili	51.87	-4.28
Newlyn	50.10	-5.54	49001	Camel	Denby	50.48	-4.80

Newport	51.55	-2.99	56001	Usk	Chainbridge	51.74	-2.95
Newport	55.01	-1.44	23003	North Tyne	Reaverhill	55.05	-2.15
Newport	51.55	-2.99	57005	Taff	Pontypridd	51.60	-3.33
Newport	51.55	-2.99	56002	Ebbw	Rhiwderin	51.59	-3.07
Newport	51.55	-2.99	57007	Taff	Fiddlers Elbow	51.65	-3.32
Newport	51.55	-2.99	57006	Rhondda	Trehafod	51.61	-3.37
Newport	51.55	-2.99	57008	Rhymney	Llanedeyrn	51.53	-3.12
North Shields	55.01	-1.44	23001	Tyne	Bywell	54.95	-1.94
North Shields	55.01	-1.44	23004	South Tyne	Haydon Bridge	54.98	-2.22
North Shields	55.01	-1.44	24009	Wear	Chester le Street	54.85	-1.56
North Shields	55.01	-1.44	24001	Wear	Sunderland Bridge	54.73	-1.59
North Shields	55.01	-1.44	23006	South Tyne	Featherstone	54.94	-2.51
North Shields	55.01	-1.44	22001	Coquet	Morwick	55.33	-1.63
North Shields	55.01	-1.44	23022	North Tyne	Uglydub	55.18	-2.45
North Shields	55.01	-1.44	23005	North Tyne	Tarset	55.17	-2.35
North Shields	55.01	-1.44	24008	Wear	Witton Park	54.67	-1.73
North Shields	55.01	-1.44	23008	Rede	Rede Bridge	55.14	-2.21
North Shields	55.01	-1.44	22009	Coquet	Rothbury	55.31	-1.89
Portpatrick	54.84	-5.12	81002	Cree	Newton Stewart	54.96	-4.48
Portpatrick	54.84	-5.12	81004	Bladnoch	Low Malzie	54.86	-4.52
Portpatrick	54.84	-5.12	81006	Water of Minnoch	Minnoch Bridge	55.04	-4.57

Portpatrick	54.84	-5.12	81003	Luce	Airyhemming	54.90	-4.84
Portrush	55.21	-6.66	203040	Lower Bann	Movanagher	54.98	-6.55
Portrush	55.21	-6.66	201010	Mourne	Drumnabuoy House	54.81	-7.46
Portrush	55.21	-6.66	203093	Main	Shane's Viaduct	54.74	-6.31
Portrush	55.21	-6.66	203010	Blackwater	Maydown Bridge	54.41	-6.74
Portrush	55.21	-6.66	201009	Owenkillew	Crosh	54.73	-7.35
Portrush	55.21	-6.66	201008	Derg	Castlederg	54.71	-7.59
Portrush	54.84	-5.12	82003	Stinchar	Balnowlart	55.11	-4.97
Portrush	55.21	-6.66	203012	Ballinderry	Ballinderry Bridge	54.66	-6.56
Portrush	55.21	-6.66	203020	Moyola	Moyola New Bridge	54.66	-6.52
Portrush	55.21	-6.66	201006	Drumragh	Campsie Bridge	54.60	-7.29
Portrush	55.21	-6.66	236005	Colebrooke	Ballindarragh Bridge	54.27	-7.49
Portrush	55.21	-6.66	202002	Faughan	Drumahoe	54.98	-7.28
Portrush	55.21	-6.66	204001	Bush	Seneirl Bridge	55.16	-6.52
Portrush	55.21	-6.66	201005	Camowen	Camowen Terrace	54.60	-7.29
Portrush	55.21	-6.66	203011	Main	Dromona	54.92	-6.37
Portrush	55.21	-6.66	203092	Main	Dunminning	54.94	-6.36
Portrush	55.21	-6.66	236007	Sillees	Drumrainey Bridge	54.31	-7.69
Portrush	55.21	-6.66	201002	Fairywater	Dudgeon Bridge	54.63	-7.37
Portrush	55.21	-6.66	203027	Braid	Ballee	54.85	-6.29
Portsmouth	50.80	-1.11	42004	Test	Broadlands	50.97	-1.50

Portsmouth	50.80	-1.11	42023	Itchen	Riverside Park	50.94	-1.37
Portsmouth	50.80	-1.11	42024	Test	Chilbolton Total	51.15	-1.45
Portsmouth	50.80	-1.11	42010	Itchen	Highbridge & Allbrook Total	50.99	-1.34
Sheerness	51.45	0.74	39001	Thames	Kingston	51.41	-0.31
Sheerness	51.45	0.74	39072	Thames	Royal Windsor Park	51.49	-0.59
Sheerness	51.45	0.74	39121	Thames	Walton	51.39	-0.42
Sheerness	51.45	0.74	39111	Thames	Staines	51.43	-0.51
Sheerness	51.45	0.74	39130	Thames	Reading	51.46	-0.97
Sheerness	51.45	0.74	39002	Thames	Days Weir	51.64	-1.18
Sheerness	51.45	0.74	39046	Thames	Sutton Courtenay	51.65	-1.25
Sheerness	51.45	0.74	39129	Thames	Farmoor	51.76	-1.36
Sheerness	51.45	0.74	39008	Thames	Eynsham	51.77	-1.35
Sheerness	51.45	0.74	40003	Medway	Teston / East Farleigh	51.25	0.45
Sheerness	51.45	0.74	39016	Kennet	Theale	51.43	-1.07
Sheerness	51.45	0.74	39079	Wey	Weybridge	51.37	-0.46
Sheerness	51.45	0.74	39104	Mole	Esher	51.38	-0.37
Sheerness	51.45	0.74	39103	Kennet	Newbury	51.40	-1.32
Tobermory	56.62	-6.06	91002	Lochy	Camisky	56.88	-5.05
Tobermory	56.62	-6.06	92001	Shiel	Shielfoot	56.76	-5.83
Tobermory	56.62	-6.06	90003	Nevis	Claggan	56.82	-5.09
Ullapool	57.90	-5.16	94001	Ewe	Poolewe	57.76	-5.61
Ullapool	57.90	-5.16	93001	Carron	New Kelso	57.43	-5.44
Ullapool	57.90	-5.16	95001	Inver	Little Assynt	58.17	-5.16
Ullapool	57.90	-5.16	95002	Broom	Inverbroom	57.81	-5.06

Weymouth	50.61	-2.45	44001	Frome	East Stoke Total	50.68	-2.19
Weymouth	50.61	-2.45	43009	Stour	Hammoon	50.93	-2.26
Weymouth	50.61	-2.45	45004	Axe	Whitford	50.75	-3.05
Whitby	54.49	-0.61	25009	Tees	Low Moor	54.49	-1.44
Whitby	54.49	-0.61	25001	Tees	Broken Scar	54.52	-1.60
Whitby	54.49	-0.61	25008	Tees	Barnard Castle	54.54	-1.93
Whitby	54.49	-0.61	25018	Tees	Middleton in Teesdale	54.62	-2.08
Whitby	54.49	-0.61	27092	Esk	Briggswath	54.46	-0.65
Wick	58.44	-3.09	6007	Ness	Ness-side	57.45	-4.26
Wick	58.44	-3.09	8006	Spey	Boat o Brig	57.55	-3.14
Wick	58.44	-3.09	4001	Conon	Moy Bridge	57.56	-4.54
Wick	58.44	-3.09	8010	Spey	Grantown	57.32	-3.61
Wick	58.44	-3.09	5003	Glass	Kerrow Wood	57.35	-4.74
Wick	58.44	-3.09	8005	Spey	Boat of Garten	57.25	-3.75
Wick	58.44	-3.09	8002	Spey	Kinrara	57.15	-3.85
Wick	58.44	-3.09	7002	Findhorn	Forres	57.61	-3.64
Wick	58.44	-3.09	5002	Farrar	Struy	57.43	-4.68
Wick	58.44	-3.09	3003	Oykel	Easter Turnaig	57.96	-4.70
Wick	58.44	-3.09	8004	Avon	Delnashaugh	57.40	-3.36
Wick	58.44	-3.09	7001	Findhorn	Shenachie	57.38	-3.95
Wick	58.44	-3.09	2001	Helmsdale	Kilphedir	58.14	-3.70
Wick	58.44	-3.09	2002	Brora	Bruachrobie	58.01	-3.88
Wick	58.44	-3.09	3002	Carron	Sgodachail	57.89	-4.55
Wick	58.44	-3.09	97002	Thurso	Halkirk	58.52	-3.49
Wick	58.44	-3.09	8013	Feshie	Feshie Bridge	57.12	-3.90
Wick	58.44	-3.09	3004	Cassley	Rosehall	57.98	-4.59
Wick	58.44	-3.09	4005	Meig	Glenmeanie	57.53	-4.87
Wick	58.44	-3.09	4003	Alness	Alness	57.70	-4.26

Wick	58.44	-3.09	8007	Spey	Invertruim	57.04	-4.16
Wick	58.44	-3.09	8009	Dulnain	Balnaan Bridge	57.30	-3.70
Wick	58.44	-3.09	4004	Blackwater	Contin	57.57	-4.59
Wick	58.44	-3.09	6009	Moriston	Levishie	57.22	-4.65
Wick	58.44	-3.09	7004	Nairn	Firhall	57.57	-3.87
Wick	58.44	-3.09	5004	Glass	Fasnakyle	57.32	-4.80
Wick	58.44	-3.09	96001	Halladale	Halladale	58.48	-3.90
Workington	54.65	-3.57	76007	Eden	Sheepmount	54.90	-2.95
Workington	54.65	-3.57	80002	Dee	Glenlochar	54.96	-3.98
Workington	54.65	-3.57	78003	Annan	Brydekirk	55.02	-3.27
Workington	54.65	-3.57	79002	Nith	Friars Carse	55.15	-3.69
Workington	54.65	-3.57	75002	Derwent	Camerton	54.66	-3.49
Workington	54.65	-3.57	77002	Esk	Canonbie	55.07	-2.94
Workington	54.65	-3.57	79006	Nith	Drumlanrig	55.27	-3.80
Workington	54.65	-3.57	75003	Derwent	Ouse Bridge	54.68	-3.24
Workington	54.65	-3.57	76003	Eamont	Udford	54.67	-2.66
Workington	54.65	-3.57	76005	Eden	Temple Sowerby	54.65	-2.61
Workington	54.65	-3.57	75005	Derwent	Portinscale	54.60	-3.16
Workington	54.65	-3.57	77003	Liddel Water	Rowanburnfoot	55.07	-2.92
Workington	54.65	-3.57	78006	Annan	Woodfoot	55.29	-3.42
Workington	54.65	-3.57	79005	Cluden Water	Fiddlers Ford	55.10	-3.68
Workington	54.65	-3.57	76015	Eamont	Pooley Bridge	54.62	-2.82
Workington	54.65	-3.57	78005	Kinnel Water	Bridgemuir	55.15	-3.43
Workington	54.65	-3.57	76008	Irthing	Greenholme	54.91	-2.80
Workington	58.44	-3.09	4006	Bran	Dosmucheran	57.60	-5.01
Workington	54.65	-3.57	80001	Urr	Dalbeattie	54.93	-3.84
Workington	54.65	-3.57	79003	Nith	Hall Bridge	55.39	-4.08

Workington	54.65	-3.57	79004	Scar Water	Capenoch	55.23	-3.82
Workington	54.65	-3.57	75004	Cocker	Southwaite Bridge	54.64	-3.35
Workington	54.65	-3.57	74005	Ehen	Braystones	54.44	-3.53

Table 2: Day of maximum dependence between high skew surges and river discharge; in number of sites and percentage of sites

Day of maximum dependence	-5	-4	-3	-2	-1	0	+1	+2	+3	+4	+5
Number of sites	0	0	0	0	42	188	50	19	21	3	3
Percentage of sites	0%	0%	0%	0%	13%	58%	15%	6%	6.4%	1%	1%

Table 3: The number of sites with joint occurrences per decade between (i) total water level and river discharge; and (ii) skew surge and river discharge.

Total number of sites with joint occurrences per decade between:	0	0-1	1-2	2-3	3-4	4-5	>5
Extreme total water level and river discharge (percentage of sites)	61 (19%)	169 (52%)	76 (23%)	17 (5%)	2 (1%)	1 (0.3%)	0
Extreme skew surge and river discharge (percentage of sites)	24 (7%)	97 (30%)	97 (30%)	56 (17%)	31 (10%)	14 (4%)	7 (2%)

Table 4: Correlation between catchment variables and: (i) the number of joint occurrences per decade between high skew surges and river discharge; and (ii) the lag day when there is the maximum number of joint occurrences between high skew surge and high river discharge. Bold text indicates statistical significance at a 95% confidence interval.

Catchment Variable	**All Sites**		**Coastal Sites**	
	Dependence	**Lag**	**Dependence**	**Lag**
BFI	**-0.50**	**0.21**	**-0.48**	0.17
Catchment Area Size	**-0.31**	**0.12**	**-0.33**	0.13
Altitude Variation	**0.16**	-0.032	**0.34**	0.17